Spring 4-2006

Implementation of Biomaterials for the Encapsulation of Sensors

Katherine Rebekah Kesler
University of Tennessee-Knoxville

William Shriver Dabbs
University of Tennessee- Knoxville

David Andrew Holmes
University of Tennessee-Knoxville

Implementation of Biomaterials for the Encapsulation of Sensors

Senior Design Report

April 28th, 2005

Submitted by:

Bill Dabbs

David Holmes

Katherine Kesler

Sheena Schaefer

INTRODUCTION

Background

Total knee arthroplasty surgical procedures currently rely heavily on the expertise of the surgeon to balance the medial and lateral ligaments, which can lead to sub-optimal outcomes for the patient. The inadequate balance of ligaments increases loading stress at the area of contact, and cyclic loading under these conditions leads to increased wear of the polyethylene insert[1] (App B, Fig 1). The wear particles generated between the femoral and tibial implants result in joint inflammation, osteolysis (bone degradation), and eventual implant loosening (App B, Fig 2). These premature complications usually require early surgical intervention for revision compared to properly balanced knees. A key interest for researchers, design specialists, and surgeons is to reliably determine *in vivo* forces within the knee without utilizing excessive assumptions. Gait analysis and mathematical modeling techniques have various methods to predict forces within the knee, but they only produce approximations[2,3].

Dr. Mohamed Mahfouz, a joint-appointed professor at the University of Tennessee and the Oak Ridge National Laboratory, is currently involved in developing pressure sensor technology to equip surgeons with a quantitative analysis of condylar pressure intra-operatively. A few surgeons today use repackaged industrial sensors for medical applications to provide rough estimates of condylar pressure. Work by Dr. Mahfouz proposes the use of microelectromechanical systems (MEMS) attached to a surgical spacer tool that would eliminate the subjective aspect of soft tissue balance[4]. The MEMS sensors will be calibrated to sense force magnitude and relay that information with the corresponding position information of the sensor wirelessly across the operating room. The MEMS consist of arrays of piezo-resistive microcantilevers to provide a more accurate solution for soft tissue balance during surgery (App B, Fig 3).

Piezo-resistive cantilevers are made of crystalline silicon, which changes resistance due to deflection of the cantilever beam. A wheatstone bridge circuit is utilized to measure the change in resistance of each individual cantilever. The voltage output from the circuit is calibrated and varies according to the change of force on the cantilever. This technology can also be implemented in other knee applications through "smart" implant design for the determination of *in vivo* forces in the knee. The knowledge of accurate forces in the post-operative artificial knee can aid in refining surgical techniques and improve implant design to reduce wear and better replicate normal joint kinematics.

Design Objectives

The objective of this design project is to determine a material and method for packaging of the electronics of a biomedical pressure sensor. This sensor will be used to provide valuable intra-operative and *in vivo* post-operative information about specific forces and stress states experienced in an artificial knee. The sensor will be exposed to appropriate interstitial fluids, but the electronics of the sensor must be protected by encapsulation in the material of choice. Design criteria for the material selection are based on properties of the sensor, its environment, loading distribution between implant components, and economic suitability for industrial use.

Previous work has shown that polymer based epoxies are the most desirable materials for packaging the sensors[5] (Dabbs, B). Epoxies are generally comprised of two essential components, a resin and a hardener. When combined in their respective component ratio, individual molecules come into contact with one another upon mixing, and cause a chemical reaction to occur. Once this exothermic reaction initiates, the epoxy begins to cure and the heat generated attempts to escape into the surrounding container. Working time until gelation occurs is determined by the sample size and the surface area relative to the epoxy thickness. For example, the larger the sample size, the faster the reaction and the greater the temperature will become. A good rule of thumb is that for every 10°C the temperature raises, the reaction rate will double and the time the mixture remains pourable, pot time, will be doubled. To control the temperature of the reaction and minimize heat transfer, the container's contact surface area should be large relative to the thickness of the material. Once the pot time has expired, the epoxy fully cures to form an irreversible rigid plastic polymer.

The main advantage of using epoxy is its amazing range of properties that offer versatile possibilities specific to each application. In this sensor encapsulation, a two-component epoxy allows the user to polymerize the material when needed. Other beneficial properties show the epoxy is mechanically strong, chemically resistant to degradation in the solid form, and highly adhesive during conversion from liquid to solid. Low viscosity epoxies are ideal to encapsulate the sensor completely, since it can flow around the sensors easily before it polymerizes. Also, the thermal coefficients should be low to avoid damage to the electrical components.

Three types of medical grade two-part epoxy from Masterbond are tested for comparison. Their selection was based on modulus, homogeneity, coefficient of thermal expansion, and sterilization compatibility. However, there are several concerns pertaining to their curing process that must be addressed. The formation of bubbles in the epoxy solution could lead to undesirable mechanical properties. Due to the size of the microcantilevers, the formation of

bubbles on or near the cantilever could change its deflection characteristics, resulting in an inaccurate force measurement. This is especially significant with the use of microcantilever sensors; small bubbles on or near the cantilever could considerably alter its deflection leading to inaccurate data representation. Various mixing and curing methods will first be tested in order to determine which epoxy and method provide the best way to eliminate air bubbles.

Image processing will be used to quantitatively determine the amount of air bubbles present. Multiple images will be taken of the surface for each epoxy sample. A MATLAB® program will then be used to determine the percentage of image covered by bubbles; approximate size relative to the total volume of epoxy. After determining the averages and standard deviations between images and sample groups, the data can be used to help determine which epoxy and cure method is most likely to minimize bubble formation. Using this method, the samples will be compared under a variety of mechanical tests. Future tests include, but are not limited to, compressive testing, calibration of encapsulated microcantilevers, as well as testing of the final encapsulated circuit design.

Design Criterion

There are several factors that will be considered in the final selection of the epoxy used for packaging sensors. The first key factors are the mechanical properties of the epoxies. Predicted *in vivo* forces from kinematic studies on the knee show approximately 35 MPa as the maximum pressure for the medial condyle[6]. Lateral pressures have been shown to be consistently less for the correctly balanced knee, so the maximum values for the medial side were taken into account in determining the maximum desired deflection of the cantilever. A 2D model of the cantilever beam with a distributed load is shown in Figure 1.

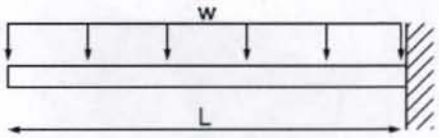

Figure 1: Two-dimensional model of cantilever loading, where "w" is the distributed load and "L" is the length.

For this application, the uniform loading assumption is valid due to the small size of the cantilever compared to the macro forces it measures on the tibial plateau.

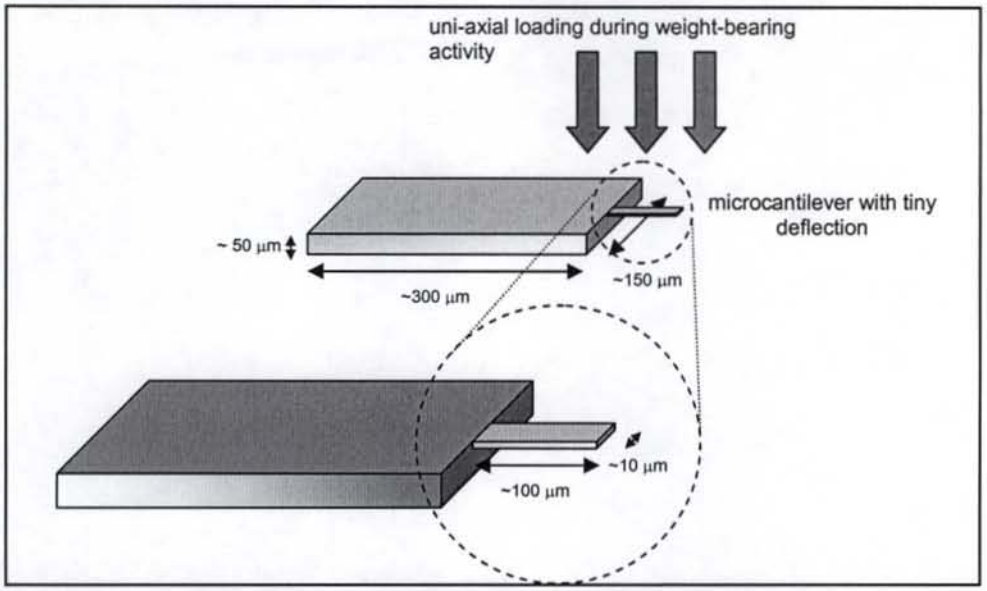

Figure 2: Microcantilever under uni-axial distributed loading with approximate dimensions

For the case of the microcantilever, the equation for the maximum deflection occurs at the free end of the cantilever and is given by

$$\delta_{MAX} = -\frac{wL^4}{8EI}. \tag{1}$$

It is assumed that an encapsulation material will decrease the deflection significantly, but the relationship between the modulus of the surrounding material and the deflection of the cantilever is difficult to determine. The sensor was subsequently modeled using finite element analysis in Coventor®. With a load of 40 MPa, which is slightly above the maximum load found in clinical studies, the simulation* indicated a deflection of 1.3 μm at the free end[6] (App. B, Fig 4). With an applied voltage of 4 volts in a wheatstone bridge (R= 1.2-1.8 kΩ), the cantilever voltage readout will change 2.3 mV for each nanometer of deflection. The sensitivity of the cantilever can be changed by changing the applied voltage. It is undesirable to use smaller applied voltages because they yield smaller changes in voltage readout. Large applied voltages are not used because they could potentially cause safety concerns for the sensor used in and around the body.

Fatigue characteristics are also important, as both the spacer and the implanted tibial tray will undergo cyclic loading. However, the loading is much higher *in vivo* for the implant than it is

* Ultra-high molecular weight polyethylene (UHMWPE) is used as the surrounding material to find a general range of deflections

for the knee lying down on the operating table during surgery[7]. Both axial and shear fatigue characteristics are important to incorporate. The material present at the articulating surface of the implant may undergo wear as the polyethylene may move in relation to the tibial tray. Initial prototype sensor designs would use only the fixed model knees, since a mobile-bearing polyethylene insert could introduce significant problems with wear.

Electrical properties are crucial to the functionality of the sensor as well. To aid in eliminating crosstalk between sensor units in an array as well as block outside noise signals, a high bulk resistivity is needed. This would prevent any significant current leakage provided that the encapsulation entirely restricts the circuitry from bodily fluids. An established dielectric constant is also important for development of capacitive sensors in the future; however, the specifications for the dielectric have not yet been established.

The effect of temperature on the circuit is also important. The material will be taken from the operating room temperature, approximately 22°C, to the human body, about 37°C. A coefficient of thermal expansion close to that of the sensor materials is needed to prevent damage to the device. Current passing through the etched copper or gold wiring layers generates additional heat and should be considered.

Fabrication is a highly important aspect of encapsulation. A major portion of this design will focus on the manufacturability and ease of use. The final material must be homogenous to allow uniform transmission of the load. For the two-part epoxies, this would include minimizing air bubbles, as they impose a change in the material behavior and the sensor embedded within. Even minor shrinkage during curing places a significant pre-stress on the cantilever, which affects the readout. The entire manufacturing process to encapsulate the sensor must be within temperatures and pressures supported by the sensor so that the circuits are not compromised. Adhesion properties of the epoxy must be capable of binding to the implant components, which include UHMWPE, CoCrMo, Ti6Al4V, and 316 L stainless steel. Any potential interaction between the epoxy and common MEMS materials such as gold, silicon, (poly) methyl-methacrylate, and copper should be minimized.

Biocompatibility is also an area of concern, since the material chosen will be exposed to surrounding tissue and fluids of the knee. Possible fluids the material may come into contact with include interstitial fluid, synovial fluid, and blood. Cells suspended in these fluids such as white blood cells, bacteria, etc. will also be in contact with the material surface. Because FDA approval is a costly and lengthy process and approval is not guaranteed, this design only tested materials that meet USP Class VI requirements. Biocompatible materials under Class VI are first

approved by compliance with USP Class V testing; the Systemic Injection Test and Intracutaneous Test compare animals' (mice and rabbits) response to sample extracts of the test materials injected and observed over a 72-hour period. Following, an Implantation Test is performed wherein test material strips and a negative control are implanted in rabbits for at least a 120-hour period. Test passage for USP Class VI is determined by macroscopic observation of hemorrhage, necrosis, discolorations, and infections, and the degree of encapsulation scored and compared with the negative control[8].

For the "smart" spacer, the exposure to soft tissues is a few seconds and will only include the superior body of the spacer, not the handle (App B, Fig 3). The surface area exposed to the body in the "smart" implant will be limited by sandwiching the sensors in the selected material between the metal (CoCrMo, Ti6Al4V, or 316L SS), tibial tray, and UHMWPE insert. Finally, the material must not degrade during at least one type of sterilization, whether ethylene oxide, gamma radiation, steam, autoclave, or chemical sterilization methods. The sensor must remain intact during the entire sterilization process.

Patent Search

In the development of a new design, a patent search must be conducted to ensure the specifications and claims do not infringe upon those rights held exclusively to the inventor of a similar preexisting "intellectual property." A patent for the encapsulation material and mechanism of MEMS sensors was searched resulting in no current designs for this application. However, a similar patent was found for *Wireless MEMS Capacitive Sensor for Physiological Parameter Measurement* (U.S. Pat. No. 6,926,670)[9]. This invention relates to an implantable microfabricated sensor device and system for measuring biologic parameters within a patient but does not include any claims regarding the specific packaging material. Although it was simply stated that the sensing device is encapsulated in a biocompatible material, this claim only supports our design criterion and hence no limitations for an encapsulation material have been presented thus far.

As a similar mechanism to measure *in vivo* forces in total knee arthroplasty, a multiaxial force-sensing implantable tibial prosthetic was developed by Orthopaedic Research Laboratories[10]. This design incorporated an internal microtransmitter for wireless data transmission through a commercially available tibial prosthetic. The microtransmitter was housed in the inner surface of a titanium alloy hollow stem by bonding the surface with transducer-grade epoxy. Forces are then determined by the voltage response of strain gauges due to the applied force distributed throughout the insert. Because this sensing system is housed within the constraints

of the prosthetic and are not exposed to interstitial fluids within the body, the components do not require complete encapsulation. Although the end use of this device is to measure in vivo forces in the knee, its approach differs in that it does not measure condylar pressure, and could therefore not be used as an indication of soft tissue balance.

MATERIALS & METHODS

Initial testing will focus on the determination of a particular epoxy and the mixing/curing method that will best meet the aforementioned design objectives. Three epoxies under consideration are EP30MED, EP42HT-2, and EP21LV. Specifications compared include, but are not limited to, mixing ratio, viscosity, working life, cure schedule, tensile strength and modulus, and bulk resistivity. The experimental design consisted of forming several groups of samples; control groups and experimental groups that varied in mixing methods, vacuum methods, and heating temperatures. For statistical significance, three similar samples of each epoxy were made for each group. Future testing with component ratios will establish an ideal elasticity, since the actual interaction of the sensor and embedding material may deviate from finite element analyses. This could be due to slight shrinkage of the epoxy during curing, or heat generated during the cure and then subsequent cooling in the stiffer environment, etc. The EP21LV, EP42HT-2, and EP30MED will be compared on the basis of the test criterion to determine which will be most ideal for sensors packaging. Technical specifications for these epoxies can be found in Appendix A.

Preliminary analysis of the material properties assumes EP30MED would provide the best results. From the technical data sheets, it has the lowest viscosity and excellent resistance to chemicals. The working life of a 100 gram mass after mixing is 30-35 minutes at 70°F which gives ample time to transfer the sample to its final container. Ultimate strength at room temperature is attained after 5-7 days with 85% of maximum strength developed within 24-48 hours, similar to that of EP21LV and EP42HT-2. The dielectric constant and coefficient of thermal expansion would have to be experimentally determined.

Many properties of EP21LV and EP42HT-2 are similar. Therefore, preparation of both epoxies under multiple variations will be needed. The EP21LV can be manipulated to have desirable mechanical characteristics based on the proportion of parts A and B in the epoxy; after curing, the material can be more rigid or more flexible, depending on the amounts used of A and B. This is especially advantageous because the exact stiffness needed for this sensor application has not been determined. The EP42HT-2 has a high tensile strength, well-defined properties, and is noted to have exceptional resistance to most types of sterilization, including gamma radiation, ethylene oxide, chemical, and steam sterilization techniques. The EP21LV and EP42HT-2 both have low coefficients of thermal expansion, which is important for a device that will go from the shelf (~22°C) to the human body (~37°C). They also have a longer working life than EP30MED after mixing at approximately 60 minutes. Another similarity is their high bulk

resistivities, which make them ideal electrical insulators. As described previously, shrinkage is a concern with all polymers listed here, since these values have not been investigated.

Experimental Procedure

Before preparing samples, environmental conditions including room temperature, atmospheric pressure, and humidity were recorded. Room temperature is an extremely important parameter to note because it will affect the curing time of the different epoxies if sufficiently high enough. It is important to keep these variables as consistent as possible so not to introduce any more variables in experimentation and testing of cure methods.

Six samples of each epoxy were completed at room temperature which was approximately 23°C. The only variable used for these six samples was mixing method. Three samples of each epoxy consisted of mixing with a magnetic stir bar, and the other three of hand mixing using a metal stir rod with a flattened, wide edge at the tip. The specific experimental procedures for each epoxy were kept consistent. The only difference existed in the ratio of Part A to B in each epoxy. The ratios for each epoxy for A to B are as follows: EP21LV 1:1, EP42HT-2 5:2, and EP30MED 4:1. Twenty gram samples were measured out with appropriate ratios of each epoxy in 100 mL beakers, with masses of each part recorded. The mass of the container and mass of mix was also recorded. Total mixing time for each mixing method was five minutes per sample. This method allowed appropriate mixing time to create a homogeneous mixture between parts A and B, and not significantly decrease working time for the samples. Once mixed, the samples were poured into plastic Petri dishes, with mass of the dish previously documented. Mass of each sample was also measured once poured into Petri dish. The epoxy samples were allowed to cure once in the dishes. Cure times for each epoxy at room temperature can be found in the technical data sheets in Appendix A.

Three samples of each epoxy were created under elevated temperature utilizing the hand mixing method with the metal stir rod. Samples performed at room temperature showed that there was no significant difference in decreasing air bubbles or creating a better mixture between hand mixing and the magnetic stir bar. Therefore, heated samples were performed using the easier mixing method, the hand mix method. Elevated temperature was used to facilitate diffusion of air bubbles within the epoxy mixture to rise to the surface. Once again, the procedure for each epoxy was kept consistent. For the EP30MED, 20 gram samples with the appropriate ratio of Part A to B were measured out in 100 mL beakers. A mixing time of five minutes was used. Once mixed, the sample was then set on a hot plate at 100 °C. The samples

were heated for five minutes, with a 30 second stir time half-way through heating. The heated samples were much less viscous, and easier to mix. After heating, the samples were poured into Petri dishes and allowed to cure. The consequence of heating decreases the working time of the epoxy as well as the cure time. It is important to find a proper temperature to heat that still allows a long enough working time to obtain a homogeneous mixture and also allows gas to escape. The same mass measurements made for the room temperature samples were also performed for the heated samples. For the EP21LV and the EP42HT-2, a significantly smaller temperature was used in heating samples. It was found that temperatures as high as 80 °C decreased working time significantly, and samples were already cured to the extent that they could not be poured into Petri dishes. Therefore 40 °C was used for heating samples of the EP21LV and the EP42HT-2. These epoxies follow the same outlined procedure for the EP30MED with the only variation in heating temperature.

A vacuum is the third variable that was to be considered in experimentation. One sample was performed using bumping, a method of fluctuating between high pressure and low pressure. Only one sample was completed using the vacuum, and gave poor results. Although permission to use a vacuum located in SERF 108 was granted, due to conflicting schedules between others needing the vacuum, no more samples were produced.

After discussions with several materials science professors, they suggested using a vacuum desiccator to try to reduce the bubbles in the samples. The equipment was found in a materials science laboratory in Dougherty. The apparatus consists of an air-tight chamber composed of two plastic hemispheres. There is a vacuum port which is connected to any laboratory vacuum line. The two hemispheres of the desiccator are sealed with a rubber o-ring, and a vacuum pull holds the two together. The vacuum desiccator holds a vacuum so that the air bubbles trapped inside of the epoxy samples. Several samples were placed under vacuum pull in the desiccator. The comparison of these samples follows in the result section.

Image Processing

In order to estimate the likelihood of bubbles forming on the micro cantilevers, it is necessary to establish a method of determining the amount of bubbles present in each sample. To accomplish this task, a probe station was used to magnify the epoxy surface and take digital images at 8x magnification. Next, the images were processed by enhancing the edges and then applying a threshold. This procedure converts the image to black and white, leaves the edges of the bubbles as white, and causes the background to become black. A MATLAB® program was then created in order to quantify the amount of the image that is covered by bubbles. The

program fills in the bubbles from the processed image with white pixels. Next, the area of the white pixels is computed. Each pixel is analyzed by looking at its two by two neighborhood. Depending on the location and number of white pixels in the pixel's neighborhood, the pixel is given a value from 0 to 1, with 0 being 4 black pixels, and 1 being 4 white pixels. These values for each pixel are summed up to give the total area of the bubbles. This area is then divided by the total area of the image (in pixels) in order to determine what percentage of the image is comprised of bubbles. This process is repeated four times for each sample, and the results are averaged to determine the total percentage score. Standard deviations are also calculated for the values. The scores can then be used to help determine quantitatively which epoxy and curing method is most suitable to encapsulate the micro cantilever sensors.

Replication of Experiment

Once it had been decided to use EP30MED, the experiment was then replicated to ensure that the results could be reproduced for EP30MED. Ten extra samples were made and analyzed using mechanical and imaging tests. The samples were produced using a 4:1 ratio for the A and B portions of the epoxy. The samples were also hand-mixed and cured without the presence of a vacuum, because this had yielded the best results so far. The ten samples provided enough data to use a simple t-test on the data to ensure statistical significance of the findings. The results and a discussion of the data follow.

Mechanical Testing of Samples

Because of the location of the epoxy on the tibia tray, several mechanical concerns need to be addressed. Due to the constant movement of the knee, the UHMW Polyethylene insert in the knee replacement will rub against the epoxy. Therefore, wear particles are of a major concern. This can cause inflammation by the bodily immune responses in the knee, but wearing can also lead to mechanical failure of the replacement itself, not to mention the circuitry. Therefore, the epoxy must be harder than the polyethylene component so that it will not wear over time. The hardness of UHMW Polyethylene is typically around ~67 on the Rockwell R Scale[11]. Samples were subjected to Rockwell hardness testing and the results follow. Due to the various loads in the knee, the epoxy will also be subjected to enormous loads. Compression testing was done in order to insure that the epoxy could withstand the load. Fourteen ~1.2cm X ~.5cm (diameter X height) cylindrical "pucks" (see geometrical data below) were molded and subjected to compression testing on the MTS 10/GL compression machine in Dougherty 217. Using MTS Test Works software, a method was written to load each epoxy sample to a maximum load of 6,000 N, and then unload to 0 N. The maximum load

chosen, 6,000 N, corresponds to five times the body weight of an approximately 270 pound individual. This amount was chosen to overestimate the amount of loading that the knee would undergo. The epoxy samples were loaded and unloaded at three different strain rates: .2 mm/s, .02 mm/s, and .002 mm/s. In order to test the failing point of the epoxy, a separate method was written to load three samples to 20,000 N and using the three different strain rates listed. However, the samples never reached this maximum loading, and began to undergo irreversible deformation. The highest loading withstood was approximately 14,500 N.

Puck	D_1	D_2	D_3	D_4	D_{ave} (in)	D (mm)	r (mm)	h (in)	h (mm)	V (mm^3)	V (m^3)
1	0.5042	0.4530	0.4790	0.4758	0.4780	12.1412	6.0706	0.2573	6.5354	756.6353	7.566E-07
2	0.5085	0.4698	0.4960	0.4920	0.4916	12.4860	6.2430	0.2255	5.7277	701.3215	7.013E-07
3	0.4955	0.4805	0.4900	0.4985	0.4911	12.4746	6.2373	0.2830	7.1882	878.5400	8.785E-07
4	0.5215	0.4620	0.4950	0.5059	0.4961	12.6009	6.3005	0.2505	6.3627	793.4822	7.935E-07
5	0.4802	0.4800	0.4860	0.4970	0.4858	12.3393	6.1697	0.2708	6.8783	822.5356	8.225E-07
6	0.5110	0.4675	0.4895	0.5052	0.4933	12.5298	6.2649	0.1941	4.9301	607.9093	6.079E-07
7	0.5227	0.4650	0.4717	0.5072	0.4917	12.4879	6.2440	0.2875	7.3025	894.4189	8.944E-07
8	0.5291	0.4685	0.4829	0.5060	0.4966	12.6143	6.3071	0.2145	5.4483	680.8877	6.809E-07
9	0.4898	0.4810	0.4905	0.4939	0.4888	12.4155	6.2078	0.2220	5.6388	682.6631	6.827E-07
10	0.5009	0.4830	0.4875	0.4948	0.4916	12.4854	6.2427	0.2960	7.5184	920.4880	9.205E-07
11	0.5000	0.4709	0.4831	0.5020	0.4890	12.4206	6.2103	0.2685	6.8199	826.3291	8.263E-07
12	0.5130	0.4645	0.4922	0.4850	0.4887	12.4123	6.2062	0.2585	6.5659	794.4962	7.945E-07
13	0.5000	0.4810	0.4980	0.4881	0.4918	12.4911	6.2455	0.1861	4.7269	579.2557	5.793E-07
14	0.4900	0.4780	0.4879	0.4850	0.4852	12.3247	6.1624	0.2861	7.2669	866.9523	8.670E-07

Puck Properties 1

RESULTS

Sample Mixing

What follows is the data from the epoxy curing methods. The sample names correspond to the manner in which they were prepared. The first numeral signifies which epoxy (21 = EP21LV, 42 = EP42HT-2, and 30 = EP30MED), the next category is the mixing method (HM = hand mixed, SB = stir bar), NV or V signifies vacuum or no-vacuum, the presence of an H means the sample was heated, the presence of a D means the sample was placed under a desiccator, and the final numeral signifies which number of that mixing method the sample is.

EP21LV	1	2	3	4	5	6	7	8
Sample	21-HM-NV-1	21-SB-NV-2	21-HM-V-1	21-HM-NV-2	21-SB-NV-2	21-HM-NV-3	21-SB-NV-3	21-SB-H-1
Date	10/15/2005	10/26/2005	11/2/2005	11/2/2005	11/11/2005	11/11/2005	11/11/2005	11/16/2005
Personnel	SS	SS,KK,BD,DH	DH,KK,SS	SS,DH	SS,DH	SS,DH	SS,DH,BD	SS,DH,BD,KK
Room Temp (°C)	23	25.5	23	23	23	22	22	23
Atmospheric Pressure (mb)	~	1022	1025.4	~	1026.8	1026	1026	1022
Humidity	29.0%	88.0%	66.0%	~	~	~	~	83.0%
Type of Stirrer	Wood	SB @ 4.75	Metal	Metal	SB @ 4.5	Metal	Stir Bar @ 4.5	Stir Bar
Mass of Mixing Container (g)	539	53.72	57.2	~	53.7	57.5	57.3	76.9
Ratio A/B	1:1	1:1	1:1	1:1	1:1	1:1	1:1	1:1
Mass Part A (g)	10.0	10.3	10.1	10.0	10.1	10.0	10.0	10.1
Mass Part B (g)	10.0	10.0	6.3	10.0	10.1	10.0	10.0	10.1
Mass Container + Mass Mix (g)	~	74	77.6	~	~	~	77.5	97.4
Mass Mix (g)	~	20.28	20.4	~	~	~	20.2	20.5
Mass of Petri Dish w/ Lid (g)	~	16.21	13.8	16.6	33.4	32.9	32.4	16.5
Mass of Mix + Petri w/ Lid (g)	~	32.65	~	34.8	~	~	~	31.7
Mass After Cure (g)	~	16.4	~	~	~	~	~	15.2
Start Time	8:27 AM	10:07 AM	11:02	12:02 PM	n/a	n/a	n/a	10:15 AM
Time End Mixing	8:31 AM	10:17 AM	11:07 AM	12:08 PM	n/a	n/a	n/a	10:31 AM
Vaccuum Pressure (mTorr)	n/a	n/a	12-250	n/a	n/a	n/a	n/a	Hood Vac
Time Placed in Vacuum	n/a	n/a	11:14-11:20	n/a	n/a	n/a	n/a	10:15-10:31
Time to Foam	n/a	n/a	11:22-11:32	n/a	n/a	n/a	n/a	n/a
Time Removed Vacuum	n/a	n/a	11:32	n/a	n/a	n/a	n/a	10:31

Mixing Method 1

EP21LV	9	10	11
Sample	21-HM-H-NV-1	21-HM-H-NV-2	21-HM-H-NV-3
Date	12/3/2005	12/3/2005	12/3/2005
Personnel	SS,KK	SS,KK	SS,KK
Room Temp (°C)	22.5	22.5	22.5
Atmospheric Pressure (mb)	1016.6	1016.6	1016.6
Humidity	91.0%	91.0%	91.0%
Type of Stirrer	HM	HM	HM
Mass of Mixing Container (g)	67.9	68.2	68.4
Ratio A/B	1:1	1:1	1:1
Mass Part A (g)	10.1	9.9	10.0
Mass Part B (g)	10.0	10.1	10.0
Mass Container + Mass Mix (g)	~	88.3	88.6
Mass Mix (g)	~	20.1	20.2
Mass of Petri Dish w/ Lid (g)	15.4	16.5	15.6
Mass of Mix + Petri w/ Lid (g)	32.5	33.3	32.9
Mass After Cure (g)	17.1	16.8	17.3
Start Time	n/a	n/a	n/a
Time End Mixing	n/a	n/a	n/a
Mix Time (min)	n/a	n/a	n/a
Vaccuum Pressure (mTorr)	n/a	n/a	n/a
Time Placed in Vacuum	n/a	n/a	n/a
Time to Foam	n/a	n/a	n/a
Time Removed Vacuum	n/a	n/a	n/a

Mixing Method 2

EP30MED	1	2	3	4	5	6	7	8
Sample	30-HM-NV-1	30-HM-NV-2	30-SB-NV-1	30-HM-NV-3	30-HM-NV-YD	30-SB-NV-2	30-HM-NV-4	30-SB-NV-3
Date	10/14/2005	10/19/2005	10/26/2005	11/2/2005	11/11/2005	11/11/2005	11/11/2005	11/11/2005
Personnel	DH	DH, KK, BD	SS,DH,KK	SS,DH	SS,DH,BD	SS,DH,BD	SS,DH,BD	SS,DH
Room Temp (°C)	23.5	23	25.5	23	22	22	22	22
Atmospheric Pressure (mb)	~	1016.9	1022	~	1026	1026	1026	1026
Humidity	~	69.0%	88.0%	~	~	~	~	~
Type of Stirrer	Metal	Metal	Large SB	Metal	Metal	SB	~	~
Mass of Mixing Container (g)	~	53.7	56.9	53.9	67.9	~	68.5	54.1
Ratio A/B	4:1	4:1	4:1	4:1	4:1	4:1	4:1	4:1
Mass Part A (g)	16.0	16.0	19.2	16.1	48.0	19.2	16.1	19.3
Mass Part B (g)	4.0	4.0	4.8	4.0	12.0	4.8	4.0	4.8
Mass Container + Mass Mix (g)	~	73.7	80.9	73.9	128.6	78	88.2	~
Mass Mix (g)	~	20	24	20	60.7	~	19.7	~
Mass of Petri Dish w/ Lid (g)	~	15.75	20	16.6	~	16.4	16.9	16.6
Mass of Mix + Petri w/ Lid (g)	~	33.61	41.9	34.5	~	38.3	32.7	38.2
Mass After Cure (g)	17.7	17.9	21.9	17.9	~	21.9	15.8	21.6
Start Time	~	10:56 AM	11:26 AM	12:27	~	~	~	~
Time End Mixing	~	11:02 AM	11:36 AM	12:33 PM	~	~	~	~
Vaccuum Pressure (mTorr)	n/a	n/a	n/a	n/a	n/a	n/a	n/a	n/a
Time Placed in Vacuum	n/a	n/a	n/a	n/a	n/a	n/a	n/a	n/a
Time to Foam	n/a	n/a	n/a	n/a	n/a	n/a	n/a	n/a
Time Removed Vacuum	n/a	n/a	n/a	n/a	n/a	n/a	n/a	n/a

Mixing Method 3

EP42HT-2	1	2	3	4	5	6	7	8	9
Sample	42-HM-NV-1	42-SB-NV-1	42-HM-NV-2	42-HM-NV-3	42-SB-NV-3	42-SB-NV-2	42-HM-H-NV-1	42-HM-H-NV-2	42-HM-H-NV-3
Date	10/15/2005	10/26/2005	11/2/2005	11/11/2005	11/11/2005	11/11/2005	12/3/2005	12/3/2005	12/3/2005
Personnel	SS	SS,DH,BD,KK	DH,SS	DH,SS,BD	BD,DH,SS	BD,SS,DH	KK,SS	KK,SS	KK,SS
Room Temp (°C)	23	25.5	23	22	22	22	22.5	22.5	22.5
Atmospheric Pressure (mb)	30.03	1022	~	1026	1026	1026	1016.6	1016.6	1016.6
Humidity	29.0%	88.0%	~	~	~	~	~	~	~
Type of Stirrer	Wood	SB	Metal	Metal	SB	SB	HM	HM	HM
Mass of Mixing Container (g)	57.1	60.2	~	71.6	63.8	57.3	68.1	67.8	68.4
Ratio A/B	5:2	5:2	5:2	5:2	5:2	5:2	5:2	5:2	5:2
Mass Part A (g)	14.3		14.3	17.1	17.1	17.0	14.3	14.3	14.5
Mass Part B (g)	5.7		5.7	6.8	6.8	6.8	5.8	5.7	5.4
Mass Container + Mass Mix (g)	~		~	95.8	78.3	81.2	~	~	~
Mass Mix (g)	~	-60.2	~	24.2	14.5	23.9	~	~	~
Mass of Petri Dish w/ Lid (g)	~		15.8	~	~	~	16.7	16.6	15.6
Mass of Mix + Petri w/ Lid (g)	~		33.4	37.9	34.5	35.5	34.2	33.5	32.7
Mass After Cure (g)	~	0.0	17.6	~	~	~	17.5	16.9	17.1
Start Time	9:04 AM	10:54 AM	12:12	n/a	n/a	n/a	n/a	n/a	n/a
Time End Mixing	9:08 AM	11:04 AM	12:18	n/a	n/a	n/a	n/a	n/a	n/a
Vaccuum Pressure (mTorr)	n/a	n/a	n/a	n/a	n/a	n/a	n/a	n/a	n/a
Time Placed in Vacuum	n/a	n/a	n/a	n/a	n/a	n/a	n/a	n/a	n/a
Time to Foam	n/a	n/a	n/a	n/a	n/a	n/a	n/a	n/a	n/a
Time Removed Vacuum	n/a	n/a	n/a	n/a	n/a	n/a	n/a	n/a	n/a

Mixing Method 4

Sample Analysis

Three mixing and curing procedures were tested for each epoxy, for a total of 27 epoxy samples. Two other mixing and curing procedures were tested, but due to time constraints, too few samples were made to ensure statistical relevance. Upon visual inspection of the samples (See Figures 3 - 5), EP30MED seems to be the most favorable epoxy to use.

(a) (b) (c)

Figure 3: Images of Epoxy Surface (Hand Mix, No Vacuum, 8x Magnification).
(a) EP21LV, (b) EP30MED, (c) EP42HT-2

(a) (b) (c)

Figure 4: Images of Epoxy Surface (Stir-Bar, No Vacuum, 8x Magnification).
(a) EP21LV, (b) EP30MED, (c) EP42HT-2

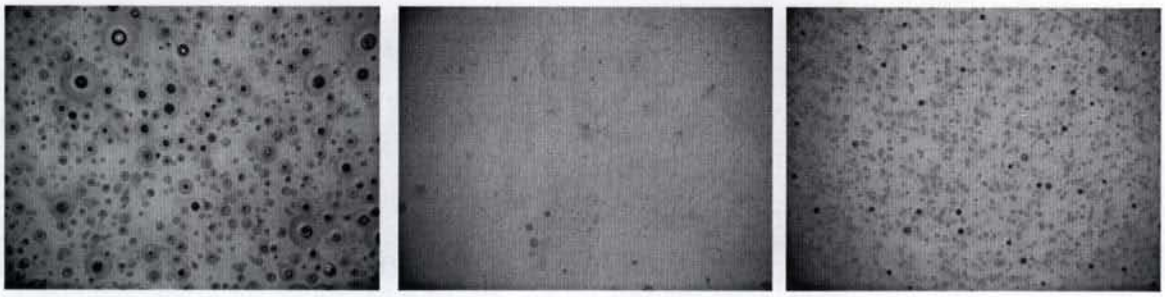

(a) (b) (c)

Figure 5: Images of Epoxy Surface (Hand Mix, Heat, No Vacuum, 8x Magnification).
(a) EP21LV, (b) EP30MED, (c) EP42HT-2

It can be seen that EP30MED contains significantly less bubbles than the other epoxies in all mixing/curing procedures. The amount of bubbles in EP42HT samples did not seem to change significantly as the mixing/curing method was varied. EP21LV experienced a very large decrease in bubbles when the stir-bar was used to mix the sample, as can be seen in figure 4(a). The sizes of the bubbles between epoxies differed greatly, as EP21LV tended to form large bubbles, while EP42HT formed a larger number of smaller bubbles. Comparing methods, the stir-bar and hand mixed samples seemed to result in a similar amount of bubbles, except for the aforementioned EP21LV. The heated samples formed more bubbles than their room-temperature counterparts. The desiccated samples fared no better with the bubbles. In fact, when the EP30MED was cured in the desiccator, more bubbles appeared. After three samples were prepared under the desiccator without producing desirable results, the procedure was scrapped. All final samples were prepared at room temperature, with no vacuum and hand-mixing.

Image Processing

Image processing results are shown in Tables 1 - 3, as well as Figure 6. Figure 6 provides an overview as to how the image is processed in order to make a bubble area determination possible. Tables 1-3 show the average and standard deviation percentage scores for the

epoxies and mixing methods.

Table 1: MATLAB® Results from Image Processing for EP21LV

EP21LV Image Processing Results		
Production Method	Total Samples	Bubble Averages
Hand Mix - No Vacuum	3	26.89% ± 9.17%
Hand Mix - Heat - No Vacuum	3	30.14% ± 17.33%
Stir Bar - No Vacuum	3	5.62% ± 3.45%

Table 2: MATLAB® Results from Image Processing for EP30MED

EP30MED Image Processing Results		
Production Method	Total Samples	Bubble Averages
Hand Mix - No Vacuum	3	1.80% ± 2.25%
Hand Mix - Heat - No Vacuum	3	2.66% ± 2.87%
Stir Bar - No Vacuum	3	2.52% ± 4.49%

Table 3: MATLAB® Results from Image Processing for EP42HT-2

EP42HT-2 Image Processing Results		
Production Method	Total Samples	Bubble Averages
Hand Mix - No Vacuum	3	17.01% ± 8.07%
Hand Mix - Heat - No Vacuum	3	24.01% ± 7.59%
Stir Bar - No Vacuum	3	23.71% ± 9.30%

The image processing results verify the results of the visual inspection of the epoxies. EP30MED contains significantly less bubbles than the other samples, with its area coverage ranging from 1.80 ± 2.25% to 2.66 ± 2.87%. EP21LV's values ranged from 5.62 ± 3.45% to 30.14 ± 17.33%, with the lower value being the stir-bar method, as indicated in the visual results. EP42HT-2 had values from 17.01 ± 8.07% to 24.01 ± 7.59%. Except for the stir-bar with EP21LV, these results indicate that EP30MED formed significantly less bubbles regardless of mixing method. Between the other epoxies, similar amounts of bubbles were formed, with EP42HT-2 having slightly lower bubble percentage values.

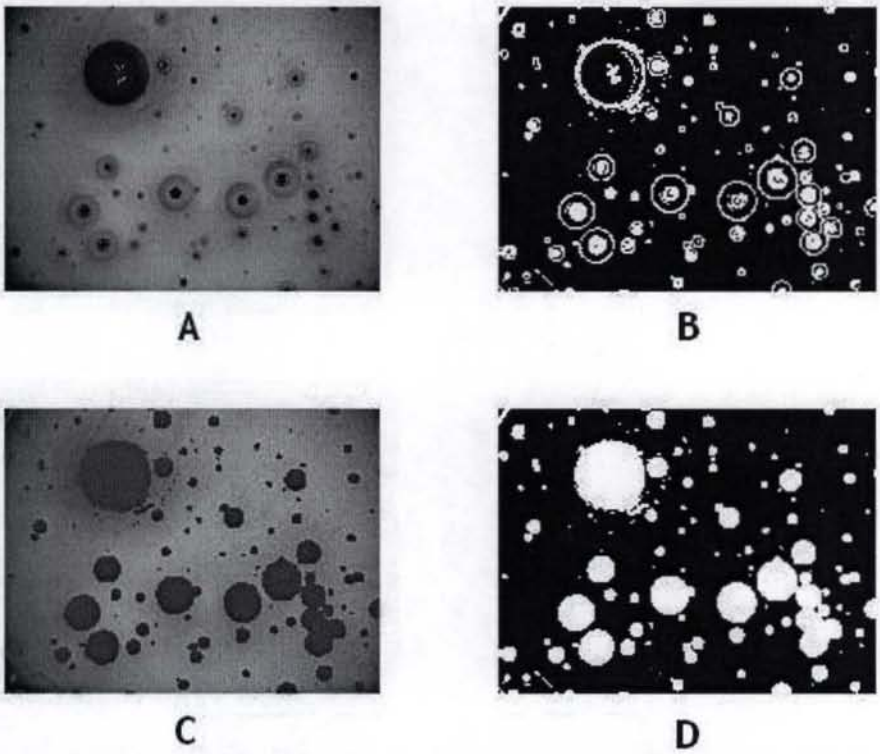

Figure 6: Image Processing Procedure Steps: (A) Original Image, (B) Edges Enhanced and Threshold Applied, (C) Filled image overlaid on original image, (D) Filled image used to calculate area.

Replication of Experiment

The experiment was replicated 11 times using the EP30MED. All of the samples were hand-mixed and cured outside of a vacuum. The methods for mixing these samples follow.

EP30MED	8	9	10	11	12	13	14	15
Sample	30-HM-H-NV-1	30-HM-H-NV-1	~	30-HM-NV-3	30-HM-D-1	30-HM-D-2	30-HM-NV-5	30-HM-NV-6
Date	12/1/2005	12/1/2005	~	12/2/2005	3/30/2006	4/4/2006	4/4/2006	4/6/2006
Personnel	KK,SS	KK,SS	KK	KK,SS	KK,BD	KK,BD	KK,BD	KK,BD
Room Temp (°C)	25.5	~	~	23	23.5	24	24	23.5
Atmospheric Pressure (mb)	~	~	~	1026.8	~	~	~	~
Humidity	~	~	~	54.0%	~	~	~	~
Type of Stirrer	HM	HM	HM	HM	HM	HM	HM	HM
Mass of Mixing Container (g)	68.7	68.2	69	53.8	68.1	57.1	68.1	68.4
Ratio A/B	4:1	4:1	4:1	~	4:1	4:1	4:1	4:1
Mass Part A (g)	16.0	16.0	16.0	16.0	12.0	15.9	16.0	11.9
Mass Part B (g)	4.1	4.0	4.0	4.0	3.0	4.1	4.2	3.1
Mass Container + Mass Mix (g)	88.4	88.3	89.2	~	83.1	77.1	88.3	~
Mass Mix (g)	19.7	20.1	20.2	~	15	20	20.2	~
Mass of Petri Dish w/ Lid (g)	16.6	16.7	15.5	16.6	15.5	16.4	16.4	16.8
Mass of Mix + Petri w/ Lid (g)	34.4	34.7	~	36.8	28.5	35.4	35.5	30.2
Mass After Cure (g)	17.8	18.0	~	20.2	13.0	19.0	19.1	13.4
Start Time	~	~	~	~	~	~	~	~
Time End Mixing	5	12:00 AM	5	5	5	5	~	~
Vaccuum Pressure (mTorr)	~	~	~	~	~	~	~	~
Time Placed in Vacuum	~	~	~	~	~	11:38 AM	~	~
Time to Foam	~	~	~	~	~	~	~	~
Time Removed Vacuum	~	~	~	~	~	~	~	~

Mixing Method 5

EP30MED	16	17	18	19	20	21	22	23	24
Sample	30-HM-NV-7	30-HM-NV-8	30-HM-NV-9	30-HM-NV-10	30-HM-NV-11	30-HM-NV-12	30-HM-NV-13	30-HM-NV-14	30-HM-NV-15
Date	4/6/2006	4/6/2006	4/11/2006	4/11/2006	4/11/2006	4/11/2006	4/11/2006	4/17/2006	4/17/2006
Personnel	KK,BD	KK,BD	KK,BD	KK,BD	KK,BD	KK,BD	KK,BD	KK,BD	KK,BD
Room Temp (°C)	23.5	23.5	23.5	23	23.5	23	23	23	23.5
Atmospheric Pressure (mb)	~	~	~	~	~	~	~	~	~
Humidity	~	~	~	~	~	~	~	~	~
Type of Stirrer	HM	HM	HM	HM	HM	HM	HM	HM	HM
Mass of Mixing Container (g)	57.8	68.2	57.1	68.1	54.1	68.3	53.8	67.7	53.5
Ratio A/B	4:1	4:1	4:1	4:1	4:1	4:1	4:1	4:1	4:1
Mass Part A (g)	12.0	16.0	17.0	12.1	24.1	12.1	12.1	12.0	12.1
Mass Part B (g)	3.0	4.0	3.0	2.9	5.9	3.0	3.0	3.0	3.0
Mass Container + Mass Mix (g)	73.7	~	~	~	~	~	~	~	~
Mass Mix (g)	15.9	~	~	~	~	~	~	~	~
Mass of Petri Dish w/ Lid (g)	16.3	16.4	16.3	16.5	16.3	16.6	16.8	15.3	16.1
Mass of Mix + Petri w/ Lid (g)	31.8	32.9	30.1	30	30.7	29.5	30.7	29	30.3
Mass After Cure (g)	15.5	16.5	13.8	13.5	14.4	12.9	13.9	13.7	14.2
Start Time	~	~	~	~	~	~	~	~	~
Time End Mixing	~	~	~	~	~	~	~	~	~
Vaccuum Pressure (mTorr)	~	~	~	~	~	~	~	~	~
Time Placed in Vacuum	~	~	~	~	~	~	~	~	~
Time to Foam	~	~	~	~	~	~	~	~	~
Time Removed Vacuum	~	~	~	~	~	~	~	~	~

Mixing Method 6

Image Processing of Replicated Samples

Imaging processing results for the replicated samples are shown below. These 11 samples were imaged randomly at seven spots on the surface. The images were processed through Adobe Photoshop and Matlab to obtain the white/black percentages. These results were then fed through JMP Statistical Software to calculate the means and t values of these tests. From this data, the outliers were removed, and the results were either accepted or rejected using a 95%

confidence interval. The JMP output is recorded in *Appendix C: Data Tables.*

Table 4: MATLAB & JMP6.0 Results from Image Processing for EP30MED Replications

EP30MED Image Processing Results												
Sample	Image	Percent White	% Minus Outliers	Mean	H_0	t	prob > |t|	Results	H_0 < 1.5	t	prob > t	Results
5	1	1.17	1.17	2.05	0	3.8060	0.0089	REJECT	1.5	1.0269	0.1720	ACCEPT
	2	0.91	0.91									
	3	1.79	1.79									
	4	3.34	3.34									
	5	0.47	0.47									
	6	2.22	2.22									
	7	4.48	4.48									
6	1	34.91	*	5.17	0	2.7560	0.0400	REJECT	1.5	1.9559	0.0539	ACCEPT
	2	1.39	1.39									
	3	0.61	0.61									
	4	3.75	3.75									
	5	10.96	10.96									
	6	10.82	10.82									
	7	3.47	3.47									
7	1	*	*	8.668	0	4.2324	0.0133	REJECT	1.5	3.500	0.0124	REJECT
	2	*	*									
	3	2.72	2.72									
	4	12.54	12.54									
	5	12.7	12.7									
	6	4.92	4.92									
	7	10.46	10.46									
8	1	1.35	1.35	2.60	0	3.8947	0.0080	REJECT	1.5	1.6465	0.0754	ACCEPT
	2	5.98	5.98									
	3	1.38	1.38									
	4	1.5	1.5									
	5	2.44	2.44									
	6	1.56	1.56									
	7	3.98	3.98									
9	1	0.17	0.17	0.94	0	3.3436	0.0205	REJECT	1.5	-2.001	0.9491	ACCEPT
	2	0.41	0.41									
	3	21.16	*									
	4	2.12	2.12									
	5	1.03	1.03									
	6	1.16	1.16									
	7	0.74	0.74									
10	1	1.63	1.63	2.61	0	5.6101	0.0025	REJECT	1.5	2.3900	0.0312	REJECT
	2	1.85	1.85									
	3	2.79	2.79									

	4	36.36	*									
	5	4.36	4.36									
	6	3.49	3.49									
	7	1.56	1.56									
11	1	10.51	10.51	12.00	0	7.5812	0.0003	REJECT	1.5	6.6339	0.0003	REJECT
	2	10.92	10.92									
	3	8.94	8.94									
	4	6.72	6.72									
	5	19.17	19.17									
	6	12.13	12.13									
	7	15.64	15.64									
12	1	*	*	1.79	0	8.765	0.0031	REJECT	1.5	1.4303	0.1240	ACCEPT
	2	*	*									
	3	2.1	2.1									
	4	1.46	1.46									
	5	2.19	2.19									
	6	27.34	*									
	7	1.42	1.42									
13	1	0.32	0.32	0.56	0	2.4947	0.0548	ACCEPT	1.5	-4.148	0.9955	ACCEPT
	2	0.25	0.25									
	3	19.8	*									
	4	0.26	0.26									
	5	1.68	1.68									
	6	0.42	0.42									
	7	0.45	0.45									
14	1	4.51	4.51	1.05	0	1.5113	0.1911	ACCEPT	1.5	-0.644	0.7261	ACCEPT
	2	0.14	0.14									
	3	0.15	0.15									
	4	*	*									
	5	0.53	0.53									
	6	0.39	0.39									
	7	0.59	0.59									
15	1	1.95	1.95	1.18	0	7.3766	0.0003	REJECT	1.5	-2.023	0.9552	ACCEPT
	2	1.44	1.44									
	3	1.28	1.28									
	4	0.77	0.77									
	5	1.08	1.08									
	6	0.95	0.95									
	7	0.77	0.77									

The preceding results show that only 2 samples of the 11 showed that a Mean Bubble Value of 0% was statistically feasible. Sample 11 was pulled from the population due to high variations from the norm. This is explained further in the discussion section. When the Mean Bubble

Value was changed from 0% to a range from 0 - 1.5%, only 2 of the 10 samples were not statistically feasible. This is a success rate change from 20% success when assuming 0% bubbles to a 80% success rate when assuming that the total bubble area would be less than 1.5% of the entire surface.

Mechanical Testing of Samples

The hardness testing of the epoxy is below. The samples were obtained by either smashing samples from the Petri dishes or using the untested intact pucks. For plastics, a Rockwell R or M scale is normally implemented. The M scale is used for harder materials and the R scale is used for softer materials. Some of the tests were done on the "plastics" setting, and some were done normally. The two tests showed little variation amongst results. Desirable results were obtained using both scales. With a mean value of 61.14 on the Rockwell M scale and a mean value of 120.31 on the Rockwell R scale, the EP30MED showed to be considerably harder than the standard hardness values of UHMW Polyethylene (67 on the Rockwell R scale). Therefore, the results are conclusive enough to say that EP30MED, mixed under the said conditions, will not produce wear particles when subjected to surface contact with UHMW Polyethylene.

Table 5: Rockwell Hardness Results for EP30MED

EP30MED Rockwell Hardness Results				
Sample	**Hardness**	**Testing**	**Scale**	**Mean**
Petri 13	49.4	Plastic	M	61.14
Petri 13	53.5	Plastic	M	
Petri 13	59.7	Plastic	M	
Petri 13	52.3	Plastic	M	
Petri 14	51.2	Plastic	M	
Petri 14	51.7	Plastic	M	
Petri 14	58.2	Plastic	M	
Petri 14	51	Plastic	M	
Petri 3	75.8	Plastic	M	
Petri 3	69	Plastic	M	
Puck 12	77.9	Plastic	M	
Puck 12	74.8	Plastic	M	
Puck 14	66	Plastic	M	
Puck 14	61.5	Plastic	M	
Puck 5	59.5	Plastic	M	
Puck 5	66.7	Plastic	M	
Petri 1	116.6	Plastic	R	120.31
Petri 1	117.9	Normal	R	

Petri 14	121.8	Plastic	R	
Petri 15	123.7	Plastic	R	
Petri 15	120.4	Plastic	R	
Petri 3	121.8	Plastic	R	
Petri 3	120	Plastic	R	

From the compression testing, loading rate did have an effect on the stress-strain relationship of the epoxy. Most deformation occurred in the slow loading rate, which had an average deformation of 0.117 mm. The medium loading rate had an average deformation of .0383 mm with the fast having an average deformation of .0228 mm. The average deformation between the three rates was 0.0594 mm. The epoxy samples undergoing the slow loading rate were loaded on average for 390 seconds. The medium average strain-rate total time was 32.3 seconds, and the fast was only 4 seconds. While the epoxy did not follow a completely linear trend, elastic modulus was calculated from the three samples that underwent a maximum load of 20,000 N. The average elastic modulus from the three tests was found to be 1.359 GPa. The Stress vs. Strain curves of these tests are located in *Appendix C: Data Tables*.

Discussion

In evaluating the suitability of the epoxies, the aforementioned design criteria were considered. From the data sheets and technical specifications, all three of the epoxies considered seemed to be suitable for our application. However, there are a number of characteristics about the various epoxies that could not be determined from the data sheets. These include the ease of mixing, how well the components mixed together, and variations due to mixing or curing procedures. After mixing and curing 27 samples of the epoxies, several conclusions were able to be drawn about mixing and curing methods, as well as the epoxies themselves. The mixing and curing properties will first be compared, followed by a comparison of the epoxies themselves.

Mixing and Curing Methods

The mixing methods did not create as large of a variation in the results as was expected. Hand mixing and stir-bar mixing proved to be roughly equivalent, except in the case of EP21LV, which experienced a large reduction in bubbles when mixed by stir-bar. Overall mixing time was more important, as mixing longer resulted in more homogenous samples. Heating the epoxy did not produce favorable results. The bubbles were more numerous, and they were distributed evenly through the surface. This distribution contrasts with the non-heated samples, as the majority of the bubbles were formed on or near the surface only (EP42HT excluded). The even distribution is most likely due to the reduced working and curing time of the heated samples, as the bubbles did not have enough time to rise to the surface and escape into the surrounding air. As the micro cantilevers are beneath the surface of the epoxy, sub-surface bubbles are more likely to interfere with its function. Due to the similarity of the results between them, either hand mixing or stir-bar mixing would be sufficient for epoxy production. Again, the desiccation of samples is not recommended for the mixing of these epoxies.

Epoxy Characteristics

In contrast to the effect of the mixing methods, the epoxies themselves greatly affected the suitability of the samples. The viscosities of the epoxies proved to be significant parameters. EP30MED mixed together easily, flowed well, and was homogeneous due to its lower viscosity. These properties, along with its minimal bubble formation, make EP30MED the easiest epoxy to work with. EP21LV was significantly more viscous, and as a result, more bubbles were introduced during mixing. Also, it was difficult to get the components to combine, and a

homogenous mixture was not always produced. Several EP21LV samples contained swirling, indicating that the components were not fully mixed. EP42HT was unique in that the individual component viscosities differed greatly. This made the epoxy difficult to mix, as the components did not initially combine well, and increased mixing time was required. However, with this increased mixing time, a homogenous mixture was able to be formed. The higher viscosity of the latter epoxies also makes it difficult for the air bubbles to escape, which helps to explain the higher bubble concentrations. Overall, EP30MED provided the best results and had the greatest ease of use.

Image Processing

From the above results for image processing, several conclusions can be drawn. EP30MED samples contained significantly less bubbles than the other epoxies. Its percentage score ranged from 1.80% to 2.66%. Visual inspection of the samples showed very few bubbles, and the majority of the samples had good optical clarity, which indicates a homogenous mixture was reached between the components. Except for the Stir-Bar method, EP42HT performed better than EP21LV, although many bubbles still remained. The compositions of the bubbles between EP42HT and EP21LV were quite different, as EP42HT formed with many small bubbles, while EP21LV tended to form with fewer bubbles, but they were significantly larger. If the stirring methods are compared, it seems that hand mixing and stir-bar mixing gave similar results. The exception to this conclusion is EP21LV, where using the stir-bar resulted in a large decrease in the number of bubbles that were formed. Heating in conjunction with hand mixing caused the bubble area to increase. This was probably due to the reduced pot time and cure time of the samples due to the increase in epoxy temperature, which did not allow enough time for the bubbles to rise to the surface.

Procession of Testing

With the above conclusion, repetitive testing commenced on the EP30MED. Overall, 15 samples of EP30MED were mixed. These were subjected to different tests in order to prove the epoxy's overall reliability in its use. The description of these sample curings are listed in Charts **Mixing Methods 5** and **Mixing Method 6**. The samples were all hand mixed at room temperature and cured without the presence of a vacuum. From ocular observation, most of the samples appeared to cure with a minimal amount of bubbles present while maintaining a homogenous mixture.

Image Processing of the Repetitive Samples

The images taken from these samples at first site looked similar. The overall surface patterns (if any) and minimal bubble formation insured the assumption of homogenous mixing and successful sample rendering. Sample 11 did not appear to be mixed well. Its data was so removed from the norm that it was completely pulled from the study. Through image analysis using the previously mentioned methods, a mean value of 2.66% white pixels was recorded for the 10 samples of EP30MED. Using JMP Statistical Software, a t-test was implemented to test the significance of the data. It found that only with 20% accuracy could it be assumed that this mixing method would produce no bubbles. However, it also proved that 80% accuracy could be enforced when a bubble population of 1.5% or less was deemed allowable.

Mechanical Testing of the Repetitive Samples

The Rockwell hardness tests proved that the EP30MED is harder than the Ultra High Molecular Weight Polyethylene. With a mean value of 120.31 on the Rockwell R scale, this clearly was higher than the standard 67 Rockwell R of UHMW Polyethylene.

From the compression tests, the differences in deformation between the three strain-rates can be attributed to a polymer's viscoelasticity which causes deformations from stress to be time-dependent. When a polymer undergoes an applied force, the load causes the bonds in polymer chains to rotate. Over time, these bonds will again unfold. If a load is applied slowly, chains in the polymer have time to unfold and stretch. However, if a load is applied rapidly, chains only stretch and bend, and the polymer appears more elastic. The slow strain-rate total time was much greater than the medium and fast rates. Deformation of the epoxy will be important when the sensor is encapsulated. It is desired that no deformation take to avoid crushing the sensors. There was an average deformation of 0.0594 mm associated with a load of 6,000 N. It can be concluded that with normal loads the knee would undergo which are roughly 2~5 times the body weight (typically ~3000N), minimal deformation would occur, and the sensors would remain intact. For the samples that were tested to the failing point, the epoxy never fractured and only continued to deform. This characteristic will be good for implantation into the body, because there should be no foreign particles breaking from the epoxy. The elastic modulus was calculated to be close to 1.359 GPa, and this is higher than the normal stresses typically found in the knee. Therefore, this epoxy should be able to withstand normal loading in the knee without fracturing and protect the encapsulated sensors.

Mechanical Testing of Future Experiments

Several types of testing must also be considered in order to ensure that the cantilever sensors will function correctly. This includes compressive testing, load calibration, strain gauge measurements, and hermiticity testing. Compressive testing will be used to determine if the epoxy can withstand the forces that it will face if implanted into the knee. A more realistic loading will be established by sandwiching the epoxy between stainless steel or cobalt chromium and a polyethylene layer. Ramp rates will be varied to determine whether or not they affect the strength of the epoxy. Load calibration must be done in order to ensure that the voltage readout of the cantilever corresponds to a certain load. This is accomplished by a series of tests involving placing a known load onto the packaged circuit and determining the output voltage associated with the load. Strain gauge testing will also be used to determine their suitability for measuring the load in non-axial directions (shear loading).

Hermeticity Testing is a failure analysis technique performed to detect ambient atmosphere leakage paths into the cavity of a hermetic package. Leakage in this context refers to the free movement of moisture and gases to and from the package cavity through openings that an otherwise perfect hermetic seal wouldn't have. The amount of leakage determines the magnitude of the hermeticity failure of the package. Loss of package hermeticity can result in internal corrosion and parametric shifts due to moisture effects. It is therefore necessary to detect hermeticity failures so that affected materials may be properly quarantined and the root cause of the problem properly addressed.

Hermeticity testing has two major categories: fine leak testing and gross leak testing. As their names imply, fine leak testing checks for package damage or defects that result in very small leakage. On the other hand, gross leak testing checks for large package damage or defects that result in gross package leakage. The methods used to conduct fine leak and gross leak testing are very different from each other therefore cannot substituted or used alone. A unit that passes gross leak testing may fail fine leak testing and visa versa. Thus, hermeticity testing method must include both fine leak and gross leak testing within the ranges applicable to small volumes for MEMS.

Conclusion

In order to determine which epoxy is most suitable for the encapsulation of micro cantilevers, several key properties were examined. Optimal mixing and curing procedures were first analyzed between the three different epoxies. From these trials, the optimal fabrication method at room temperature and hand mixing was determined. After analysis with image processing among the three epoxies, EP30MED was chosen based upon its ease for fabrication due to low viscosity and best yield for minimal bubble formation. This will hopefully ensure that the micro cantilevers will not produce inaccurate readings due to adhering bubbles. Once the epoxy was chosen, the experiment was replicated multiple times to attempt to produce similar results. The material properties were tested for further validation of EP30MED. The physical properties examined were hardness and compressive strength. These two key mechanical properties were examined based upon the location and application of the epoxy. The epoxy, when implanted in the knee, will be undergoing compressive loading while also being in contact with the polyethylene insert. Good wear and strength are desirable for protection of the sensors. Future work will include mechanical testing with the encapsulated sensors. From this project, the epoxy chosen will hopefully allow for sensors to produce accurate readings.

Special Thanks

We would like to thank Mike West for all of his help in our mechanical testing. We would also like to thank Emily Pritchard for her previous work on this project.

REFERENCES

1. Conditt MA, Ismaily SK, Alexander JW, Noble PC. Backside wear of modular ultra-high molecular weight polyethylene tibial inserts. J. Bone Joint Surg. Am. 2004 May;86-A(5):1031-7.
2. Guess TM, Maletsky LP. Computational modelling of a total knee prosthetic loaded in a dynamic knee simulator. Med Eng Phys. 2005 Jun;27(5):357-67.
3. Halloran JP, Petrella AJ, Rullkoetter PJ. Explicit finite element modeling of total knee replacement mechanics. J. Biomech. 2005 Feb;38(2):323-31.
4. To, G, Mahfouz M, Pritchard E. Ligament balancing during total knee arthroplasty with wireless encapsulated microcantilever strain sensors. Intl. Conf. on Biomed. Engr. Proceedings, Singapore, 2005.
5. Dabbs B, Holmes D, Kesler K, Pritchard E, Schaefer S. Material selection for biomedical application of microelectromechanical sensors. Biomaterials Science Report, University of Tennessee, 2005
6. Sharma, Adrija. A Method to Calculate the Femoro-Polyethylene Contact Pressures in Total Knee Arthroplasty In-Vivo. Master's Thesis, University of Tennessee, 2005.
7. Villa T, Migliavacca F, Gastaldi D, Colombo M, Pietrabissa R. Contact stresses and fatigue life in a knee prosthesis: comparison between in vitro measurements and computational simulations. J. Biomech. 2004 Jan;37(1):45-53.
8. Frequently asked questions about Dow Corning brand Class VI elastomers. Dow Corning Healthcare. www.dowcorning.com
9. Dabbs B, Holmes D, Kesler K, Pritchard E, Schaefer S. Material selection for biomedical application of microelectromechanical sensors. Biomaterials Science Report, University of Tennessee, 2005
10. Kirking B, Krevolin J, Townsend C, Colwell Jr CW, D'Lima DD. A multiaxial force-sensing implantable tibial prosthesis. J. Biomech. 2005 July 13 [EPub ahead of print]
11. UHMW Polyethylene, San Diego Plastics, INC. http://www.sdplastics.com/polyeth.html

Appendix A:

Technical Specifications

Appendix A: Technical Specifications

Chart 1: Master Bond EP30 Medical (two-component epoxy)

Viscosity, part A	600-700 cps
Viscosity, part B	400 cps
Tensile strength	>9500 psi
Coefficient of thermal expansion	unspecified
Bulk resistivity	$>10^{14}$ ¤-cm
Dielectric constant	unspecified
Hardness	unspecified
Shelf life	1 year
Working time after mixing	~30 minutes
Cure time @ room temp	1-2 days @ 85%; 5-7 days max strength
Working temperature range (after cure)	-60°F to 250°F

Chart 2: Master Bond EP42HT-2 (two-component epoxy)

Viscosity, mixed	3500 cps
Tensile strength	>12,000 psi
Coefficient of thermal expansion	35-40 in/in*10^{-6}/°C
Bulk resistivity	$>10^{14}$ ¤-cm
Dielectric constant	3.8
Hardness (Shore D)	>75
Shelf life	6 months
Working time after mixing	45-60 minutes
Cure time @ room temp	24-48 hrs
Working temperature range (after cure)	-60°F to 450°F

Chart 3: Master Bond EP21LV (two-component epoxy)

Viscosity, mixed	7000-8000 cps
Tensile strength	7600 psi
Coefficient of thermal expansion	53 in/in*10^{-6}/°C
Bulk resistivity	10^{15} ¤-cm
Dielectric constant	2.89
Hardness (Shore D)	>70
Shelf life	6 months
Working time after mixing	60-75 minutes
Cure time @ room temp	24-48 hours
Working temperature range (after cure)	-65°F to 250°F

Appendix B

Figures

Appendix B: Figures

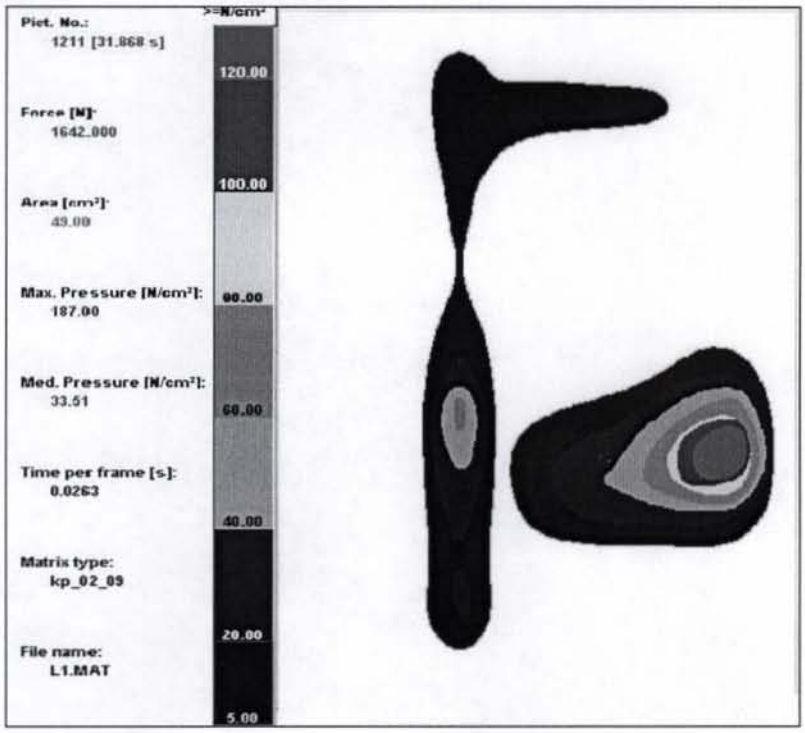

Figure 1: Improper ligament balancing can lead to increased loading at condyle contact nearest the side in greater tension. The uneven distribution of pressure signals for release of the tight side.

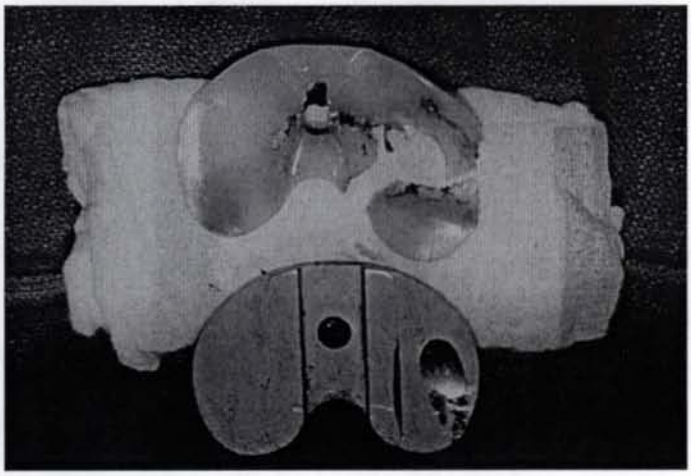

Figure 2: Catastrophic wear of polyethylene insert and tibial component as a result of improper lateral and medial ligament balancing.

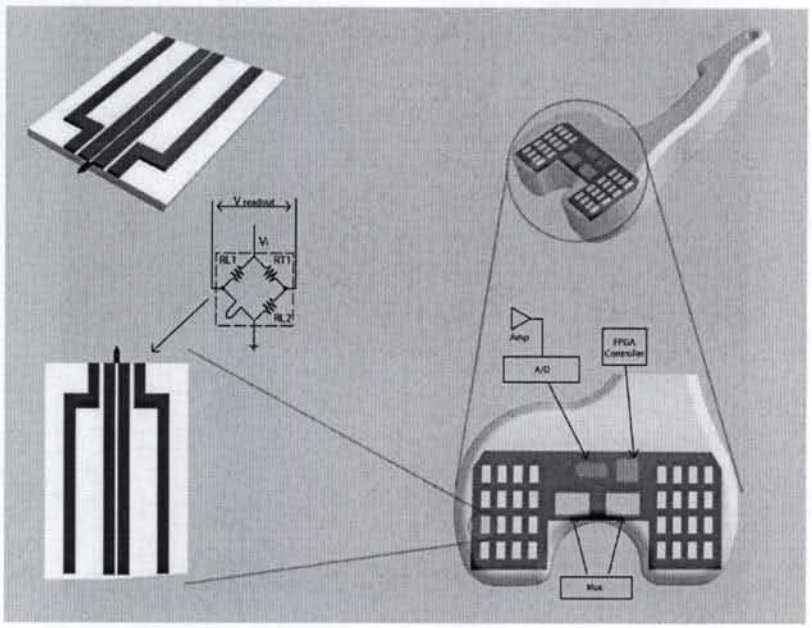

FIGURE 3: AN EXAMPLE OF A "SMART" COMPONENT DESIGN THROUGH THE INTRA-OPERATIVE APPLICATION OF A SURGICAL SPACER TOOL WITH PIEZO-RESISTIVE MICROCANTILEVER ARRAYS.

FIGURE 4: COVENTOR DEFLECTION ANALYSIS FOR A MICROCANTILEVER SUBJECTED TO LOADING.

APPENDIX C

DATA TABLES

Sample 5

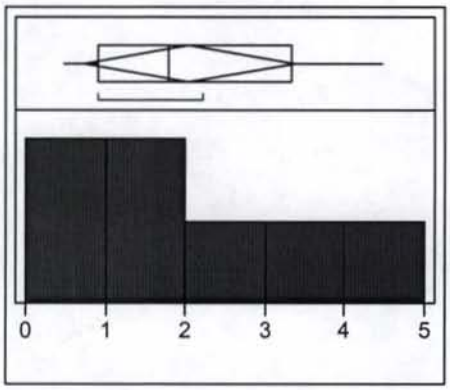

Quantiles

100.0%	maximum	4.4800
99.5%		4.4800
97.5%		4.4800
90.0%		4.4800
75.0%	quartile	3.3400
50.0%	median	1.7900
25.0%	quartile	0.9100
10.0%		0.4700
2.5%		0.4700
0.5%		0.4700
0.0%	minimum	0.4700

Moments

Mean	2.0542857
Std Dev	1.4280389
Std Err Mean	0.539748
upper 95% Mean	3.3750015
lower 95% Mean	0.73357
N	7

Test Mean=value

Hypothesized Value	0
Actual Estimate	2.05429
df	6
Std Dev	1.42804

	t Test
Test Statistic	3.8060
Prob > |t|	0.0089
Prob > t	0.0045
Prob < t	0.9955

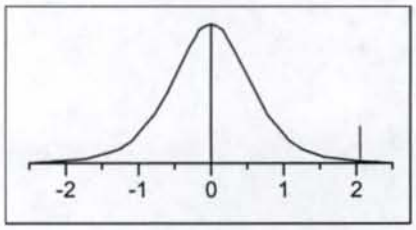

Sample 6

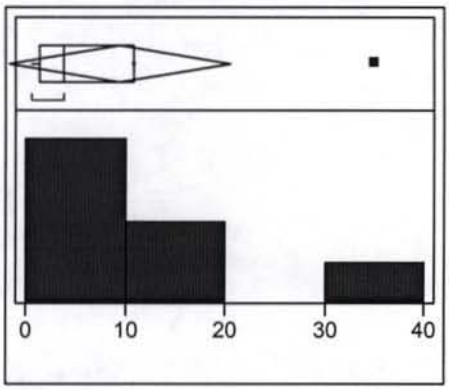

Quantiles

100.0%	maximum	34.910
99.5%		34.910
97.5%		34.910
90.0%		34.910
75.0%	quartile	10.960
50.0%	median	3.750
25.0%	quartile	1.390
10.0%		0.610
2.5%		0.610
0.5%		0.610
0.0%	minimum	0.610

Moments

Mean	9.4157143
Std Dev	11.998055
Std Err Mean	4.5348386
upper 95% Mean	20.512065
lower 95% Mean	-1.680636
N	7

Test Mean=value

Hypothesized Value	0
Actual Estimate	9.41571
df	6
Std Dev	11.9981

	t Test
Test Statistic	2.0763
Prob > |t|	0.0832
Prob > t	0.0416
Prob < t	0.9584

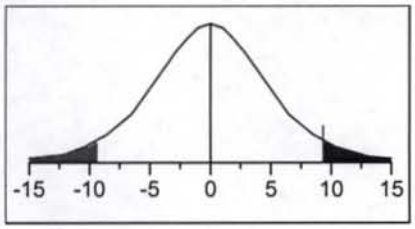

Sample 6 Without Outliers

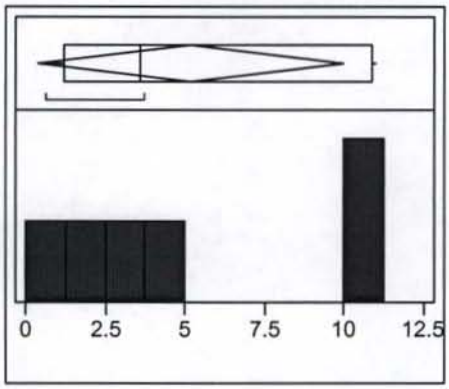

Quantiles

100.0%	maximum	10.960
99.5%		10.960
97.5%		10.960
90.0%		10.960
75.0%	quartile	10.855
50.0%	median	3.610
25.0%	quartile	1.195
10.0%		0.610
2.5%		0.610
0.5%		0.610
0.0%	minimum	0.610

Moments

Mean	5.1666667
Std Dev	4.5920569
Std Err Mean	1.8746994
upper 95% Mean	9.9857348
lower 95% Mean	0.3475985
N	6

Test Mean=value

Hypothesized Value	0
Actual Estimate	5.16667
df	5
Std Dev	4.59206

	t Test
Test Statistic	2.7560
Prob > |t|	0.0400
Prob > t	0.0200
Prob < t	0.9800

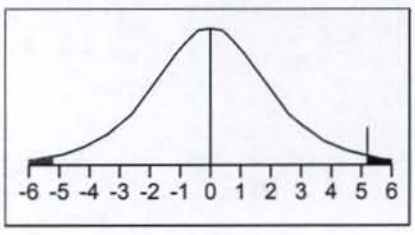

Sample 7

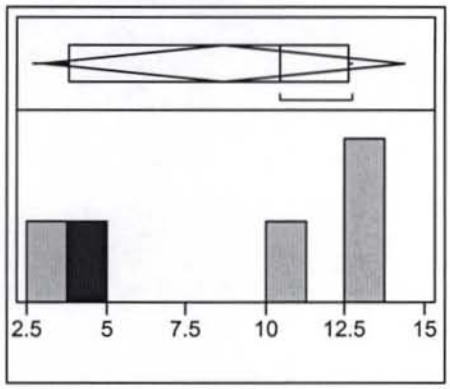

Quantiles

100.0%	maximum	12.700
99.5%		12.700
97.5%		12.700
90.0%		12.700
75.0%	quartile	12.620
50.0%	median	10.460
25.0%	quartile	3.820
10.0%		2.720
2.5%		2.720
0.5%		2.720
0.0%	minimum	2.720

Moments

Mean	8.668
Std Dev	4.5794891
Std Err Mean	2.0480098
upper 95% Mean	14.354187
lower 95% Mean	2.9818133
N	5

Test Mean=value

Hypothesized Value	0
Actual Estimate	8.668
df	4
Std Dev	4.57949

	t Test
Test Statistic	4.2324
Prob > |t|	0.0133
Prob > t	0.0067
Prob < t	0.9933

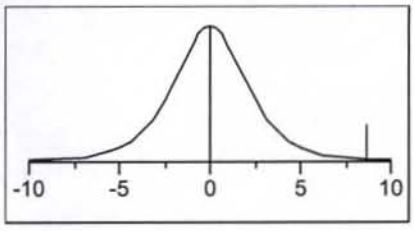

Sample 8

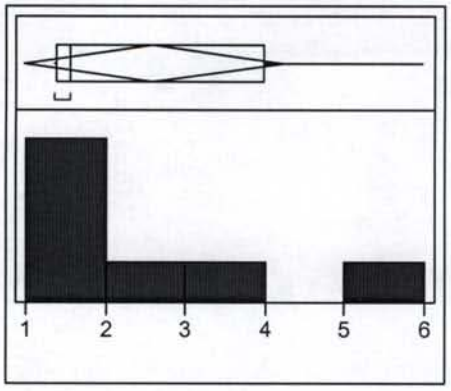

Quantiles

100.0%	maximum	5.9800
99.5%		5.9800
97.5%		5.9800
90.0%		5.9800
75.0%	quartile	3.9800
50.0%	median	1.5600
25.0%	quartile	1.3800
10.0%		1.3500
2.5%		1.3500
0.5%		1.3500
0.0%	minimum	1.3500

Moments

Mean	2.5985714
Std Dev	1.7652613
Std Err Mean	0.6672061
upper 95% Mean	4.2311659
lower 95% Mean	0.965977
N	7

Test Mean=value

Hypothesized Value	0
Actual Estimate	2.59857
df	6
Std Dev	1.76526

	t Test
Test Statistic	3.8947
Prob > |t|	0.0080
Prob > t	0.0040
Prob < t	0.9960

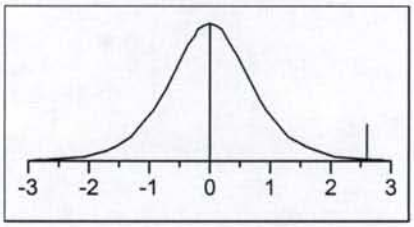

Sample 9

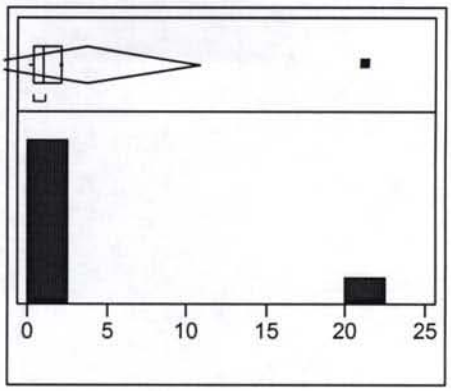

Quantiles

100.0%	maximum	21.160
99.5%		21.160
97.5%		21.160
90.0%		21.160
75.0%	quartile	2.120
50.0%	median	1.030
25.0%	quartile	0.410
10.0%		0.170
2.5%		0.170
0.5%		0.170
0.0%	minimum	0.170

Moments

Mean	3.8271429
Std Dev	7.6687889
Std Err Mean	2.8985298
upper 95% Mean	10.91959
lower 95% Mean	-3.265304
N	7

Test Mean=value

Hypothesized Value	0
Actual Estimate	3.82714
df	6
Std Dev	7.66879

	t Test
Test Statistic	1.3204
Prob > |t|	0.2348
Prob > t	0.1174
Prob < t	0.8826

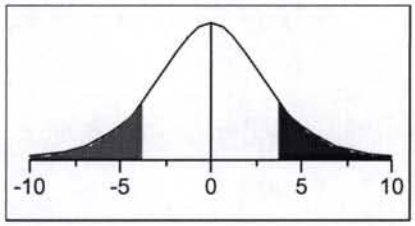

Sample 9 - Outliers

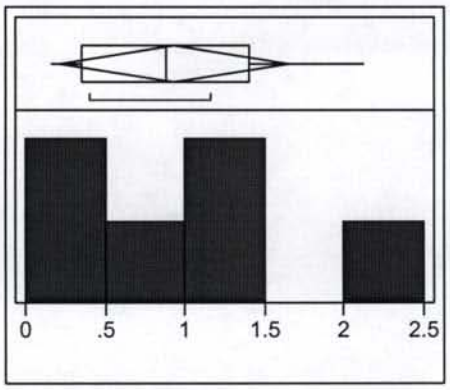

Quantiles

100.0%	maximum	2.1200
99.5%		2.1200
97.5%		2.1200
90.0%		2.1200
75.0%	quartile	1.4000
50.0%	median	0.8850
25.0%	quartile	0.3500
10.0%		0.1700
2.5%		0.1700
0.5%		0.1700
0.0%	minimum	0.1700

Moments

Mean	0.9383333
Std Dev	0.687413
Std Err Mean	0.2806352
upper 95% Mean	1.6597291
lower 95% Mean	0.2169376
N	6

Test Mean=value

Hypothesized Value	0
Actual Estimate	0.93833
df	5
Std Dev	0.68741

	t Test
Test Statistic	3.3436
Prob > |t|	0.0205
Prob > t	0.0102
Prob < t	0.9898

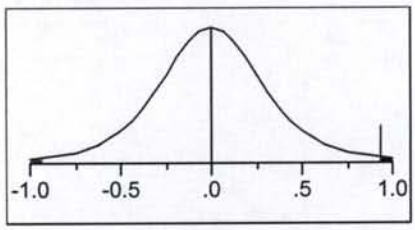

Sample 10

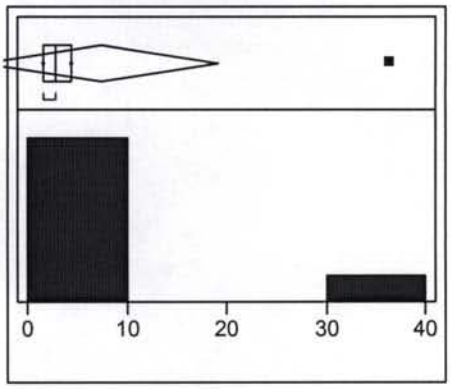

Quantiles

100.0%	maximum	36.360
99.5%		36.360
97.5%		36.360
90.0%		36.360
75.0%	quartile	4.360
50.0%	median	2.790
25.0%	quartile	1.630
10.0%		1.560
2.5%		1.560
0.5%		1.560
0.0%	minimum	1.560

Moments

Mean	7.4342857
Std Dev	12.797501
Std Err Mean	4.8370007
upper 95% Mean	19.27
lower 95% Mean	-4.401429
N	7

Test Mean=value

Hypothesized Value	0
Actual Estimate	7.43429
df	6
Std Dev	12.7975

	t Test
Test Statistic	1.5370
Prob > |t|	0.1752
Prob > t	0.0876
Prob < t	0.9124

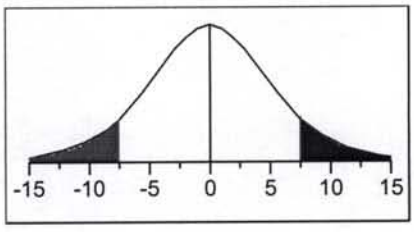

Sample 10 - Outliers

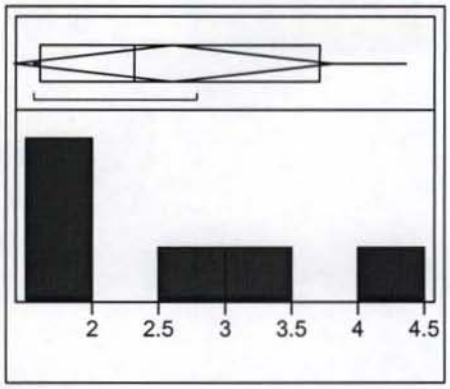

Quantiles

100.0%	maximum	4.3600
99.5%		4.3600
97.5%		4.3600
90.0%		4.3600
75.0%	quartile	3.7075
50.0%	median	2.3200
25.0%	quartile	1.6125
10.0%		1.5600
2.5%		1.5600
0.5%		1.5600
0.0%	minimum	1.5600

Moments

Mean	2.6133333
Std Dev	1.1410288
Std Err Mean	0.465823
upper 95% Mean	3.8107696
lower 95% Mean	1.4158971
N	6

Test Mean=value

Hypothesized Value	0
Actual Estimate	2.61333
df	5
Std Dev	1.14103

	t Test
Test Statistic	5.6101
Prob > |t|	0.0025
Prob > t	0.0012
Prob < t	0.9988

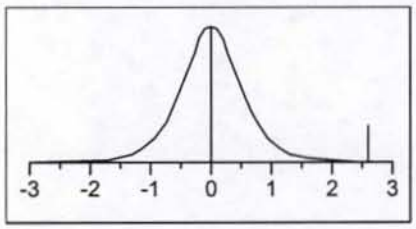

Sample 11

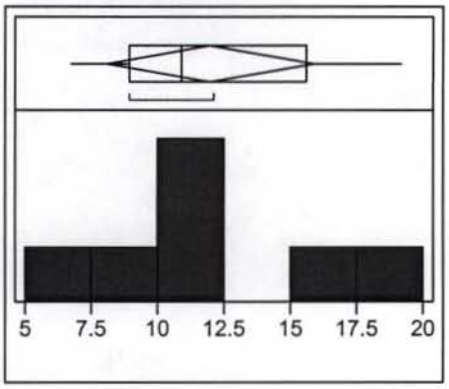

Quantiles

100.0%	maximum	19.170
99.5%		19.170
97.5%		19.170
90.0%		19.170
75.0%	quartile	15.640
50.0%	median	10.920
25.0%	quartile	8.940
10.0%		6.720
2.5%		6.720
0.5%		6.720
0.0%	minimum	6.720

Moments

Mean	12.004286
Std Dev	4.189347
Std Err Mean	1.5834243
upper 95% Mean	15.878786
lower 95% Mean	8.1297859
N	7

Test Mean=value

Hypothesized Value	0
Actual Estimate	12.0043
df	6
Std Dev	4.18935

	t Test
Test Statistic	7.5812
Prob > |t|	0.0003
Prob > t	0.0001
Prob < t	0.9999

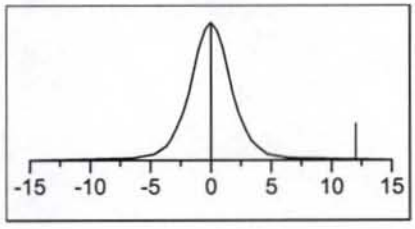

Sample 12

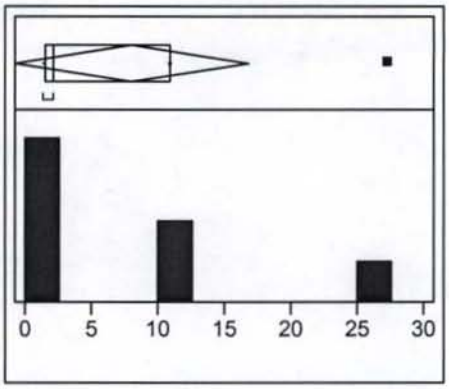

Quantiles

100.0%	maximum	27.340
99.5%		27.340
97.5%		27.340
90.0%		27.340
75.0%	quartile	10.950
50.0%	median	2.190
25.0%	quartile	1.460
10.0%		1.420
2.5%		1.420
0.5%		1.420
0.0%	minimum	1.420

Moments

Mean	7.9842857
Std Dev	9.5155607
Std Err Mean	3.5965439
upper 95% Mean	16.784712
lower 95% Mean	-0.81614
N	7

Test Mean=value

Hypothesized Value	0
Actual Estimate	7.98429
df	6
Std Dev	9.51556

	t Test
Test Statistic	2.2200
Prob > |t|	0.0682
Prob > t	0.0341
Prob < t	0.9659

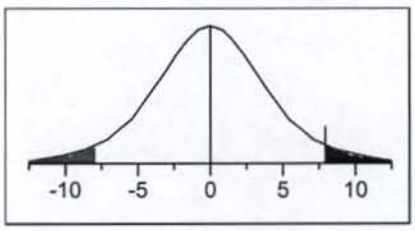

Sample 12 - Outliers

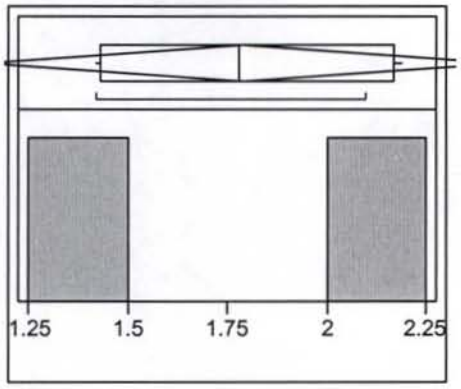

Quantiles

100.0%	maximum	2.1900
99.5%		2.1900
97.5%		2.1900
90.0%		2.1900
75.0%	quartile	2.1675
50.0%	median	1.7800
25.0%	quartile	1.4300
10.0%		1.4200
2.5%		1.4200
0.5%		1.4200
0.0%	minimum	1.4200

Moments

Mean	1.7925
Std Dev	0.409013
Std Err Mean	0.2045065
upper 95% Mean	2.443331
lower 95% Mean	1.141669
N	4

Test Mean=value

Hypothesized Value	0
Actual Estimate	1.7925
df	3
Std Dev	0.40901

	t Test
Test Statistic	8.7650
Prob > |t|	0.0031
Prob > t	0.0016
Prob < t	0.9984

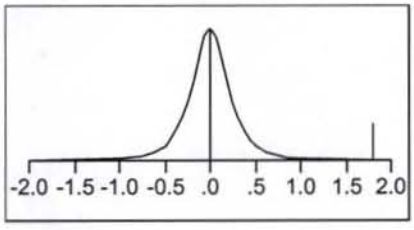

Sample 14

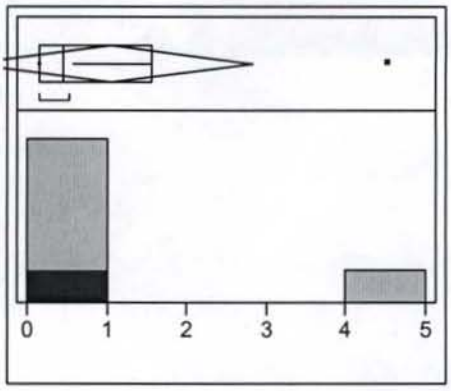

Quantiles

100.0%	maximum	4.5100
99.5%		4.5100
97.5%		4.5100
90.0%		4.5100
75.0%	quartile	1.5700
50.0%	median	0.4600
25.0%	quartile	0.1475
10.0%		0.1400
2.5%		0.1400
0.5%		0.1400
0.0%	minimum	0.1400

Moments

Mean	1.0516667
Std Dev	1.70454
Std Err Mean	0.6958755
upper 95% Mean	2.8404717
lower 95% Mean	-0.737138
N	6

Test Mean=value

Hypothesized Value	0
Actual Estimate	1.05167
df	5
Std Dev	1.70454

	t Test
Test Statistic	1.5113
Prob > |t|	0.1911
Prob > t	0.0956
Prob < t	0.9044

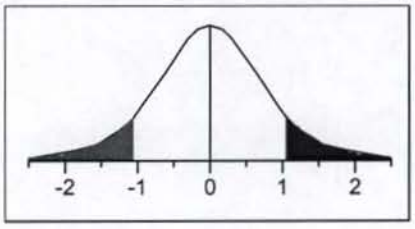

Sample 15

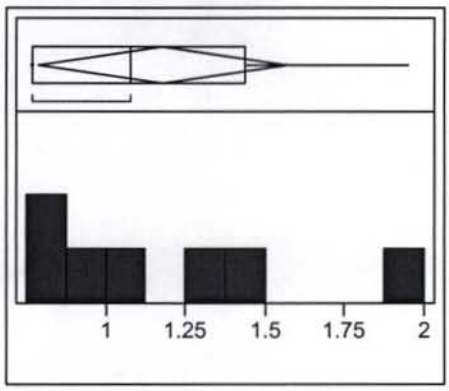

Quantiles

100.0%	maximum	1.9500
99.5%		1.9500
97.5%		1.9500
90.0%		1.9500
75.0%	quartile	1.4400
50.0%	median	1.0800
25.0%	quartile	0.7700
10.0%		0.7700
2.5%		0.7700
0.5%		0.7700
0.0%	minimum	0.7700

Moments

Mean	1.1771429
Std Dev	0.4222051
Std Err Mean	0.1595785
upper 95% Mean	1.5676174
lower 95% Mean	0.7866683
N	7

Test Mean=value

Hypothesized Value	0
Actual Estimate	1.17714
df	6
Std Dev	0.42221

	t Test
Test Statistic	7.3766
Prob > |t|	0.0003
Prob > t	0.0002
Prob < t	0.9998

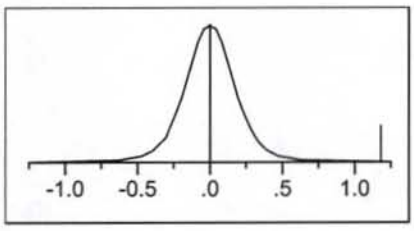

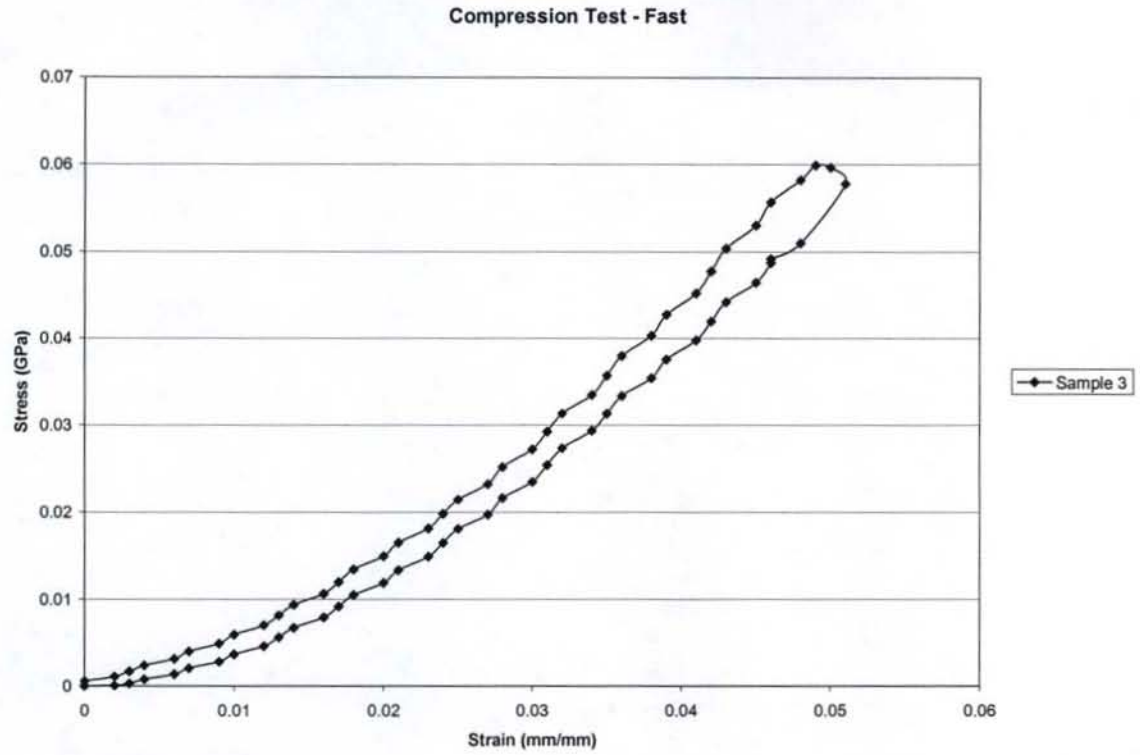

Figure 1 - 7.188 mm thickness

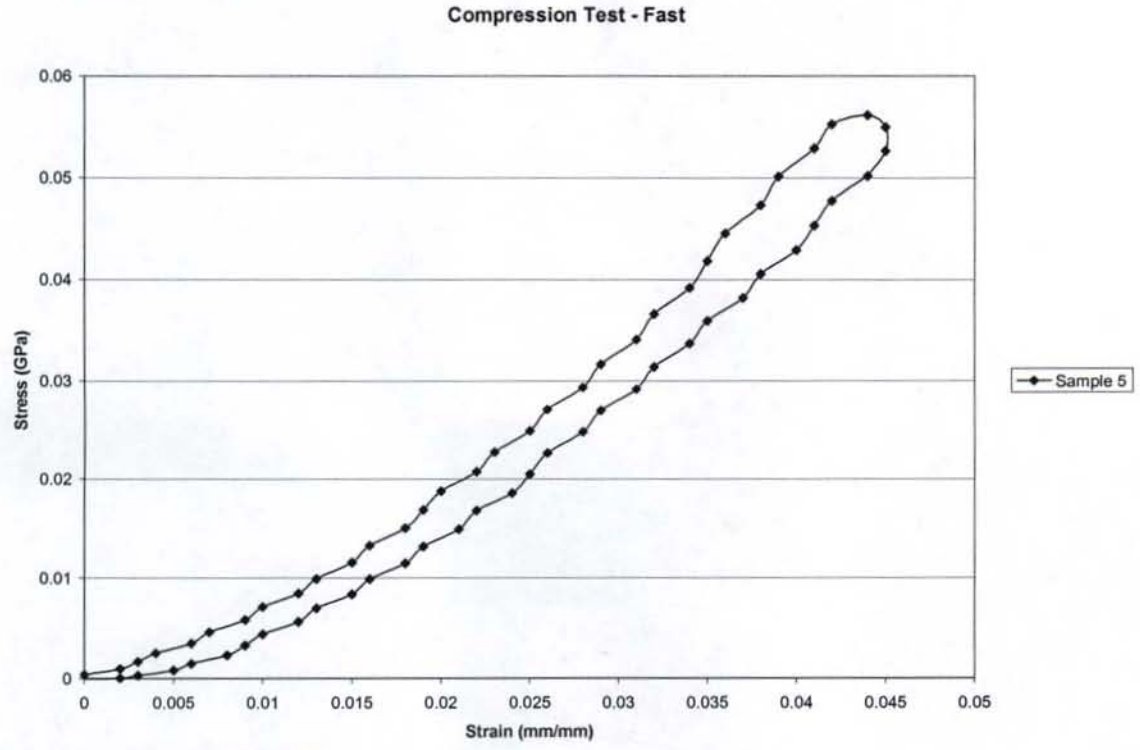

Figure 2 – 6.878 mm thickness

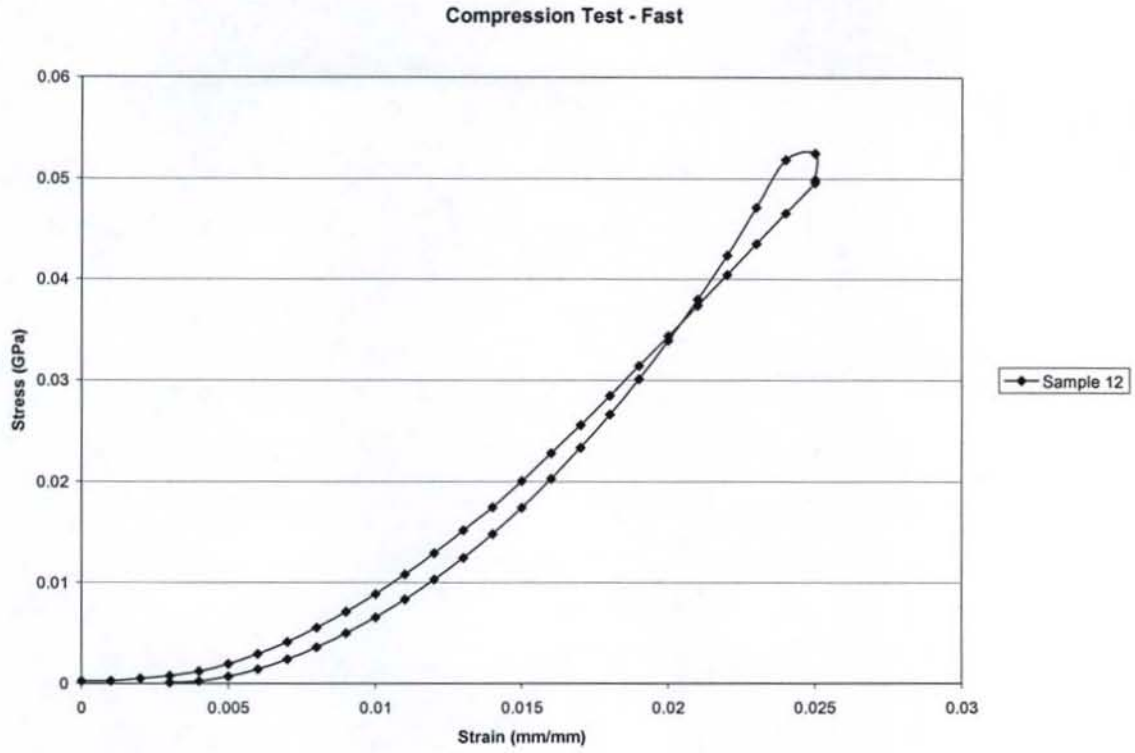

Figure 3 - 6.566 mm thickness

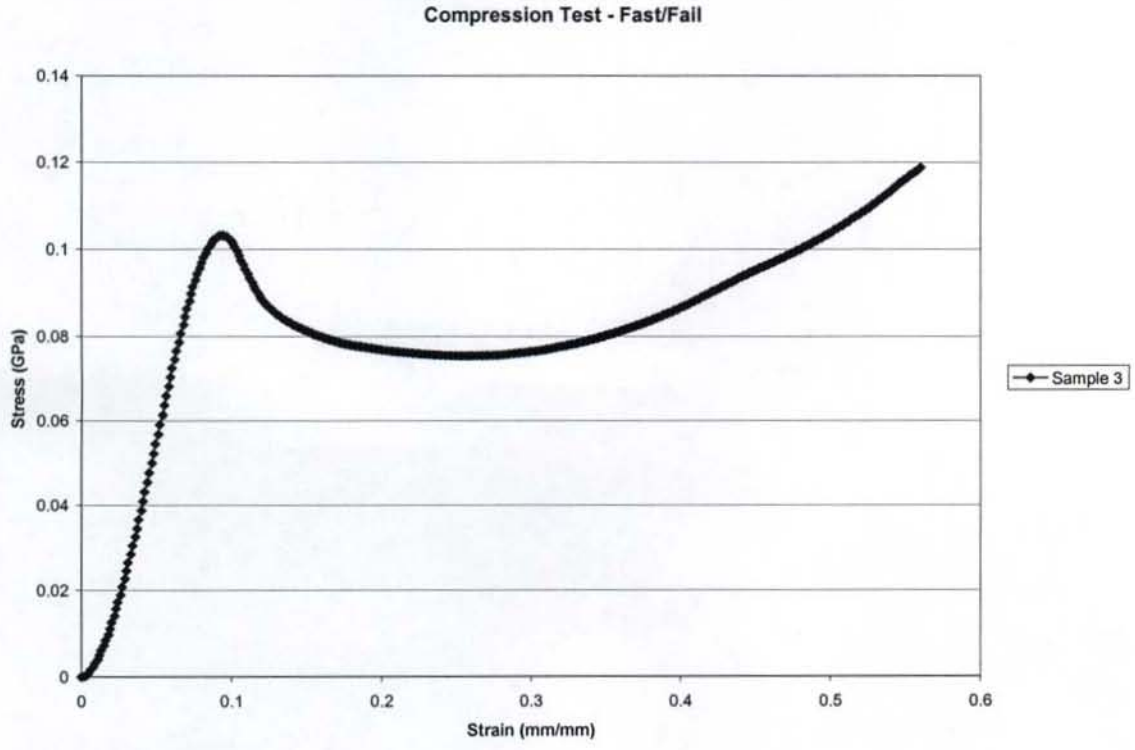

Figure 4 – 7.188 mm thickness

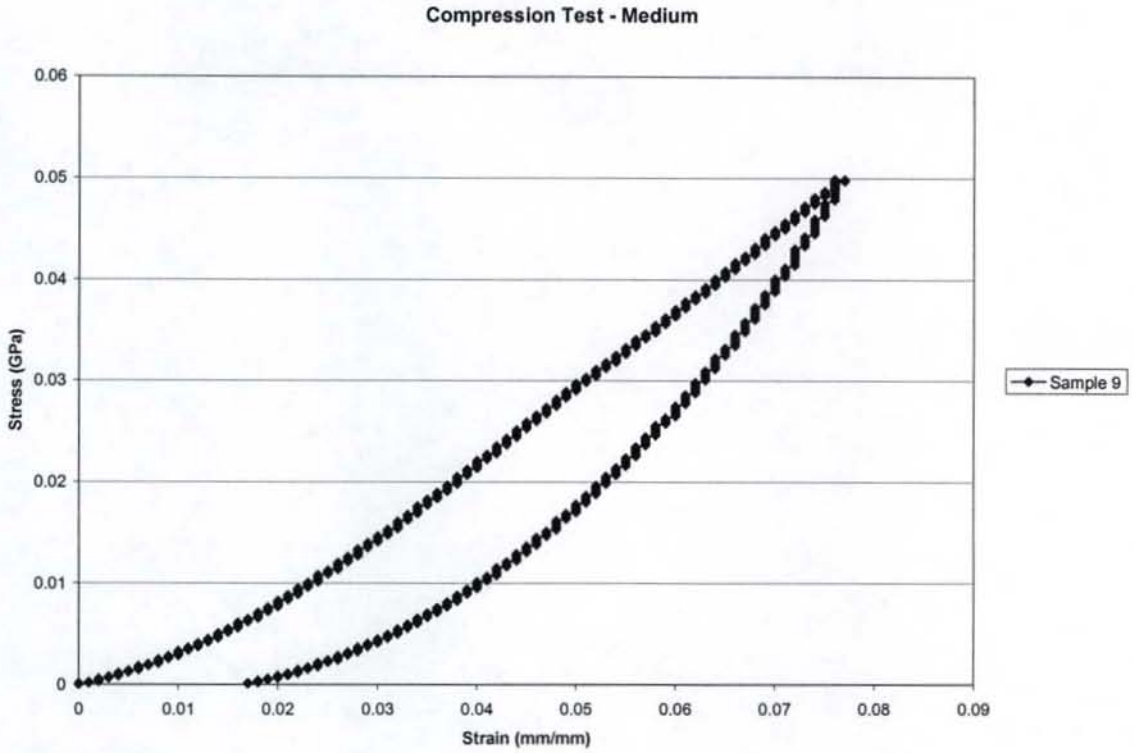

Figure 5 – 5.639 mm thickness

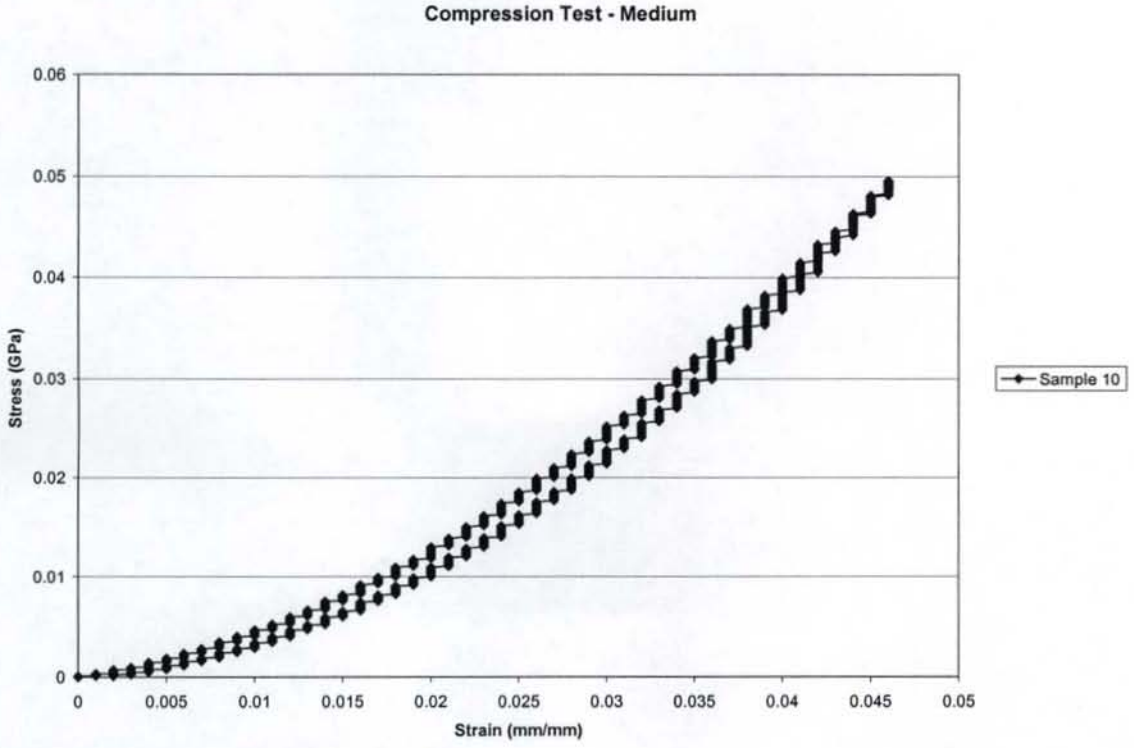

Figure 6 – 7.518 mm thickness

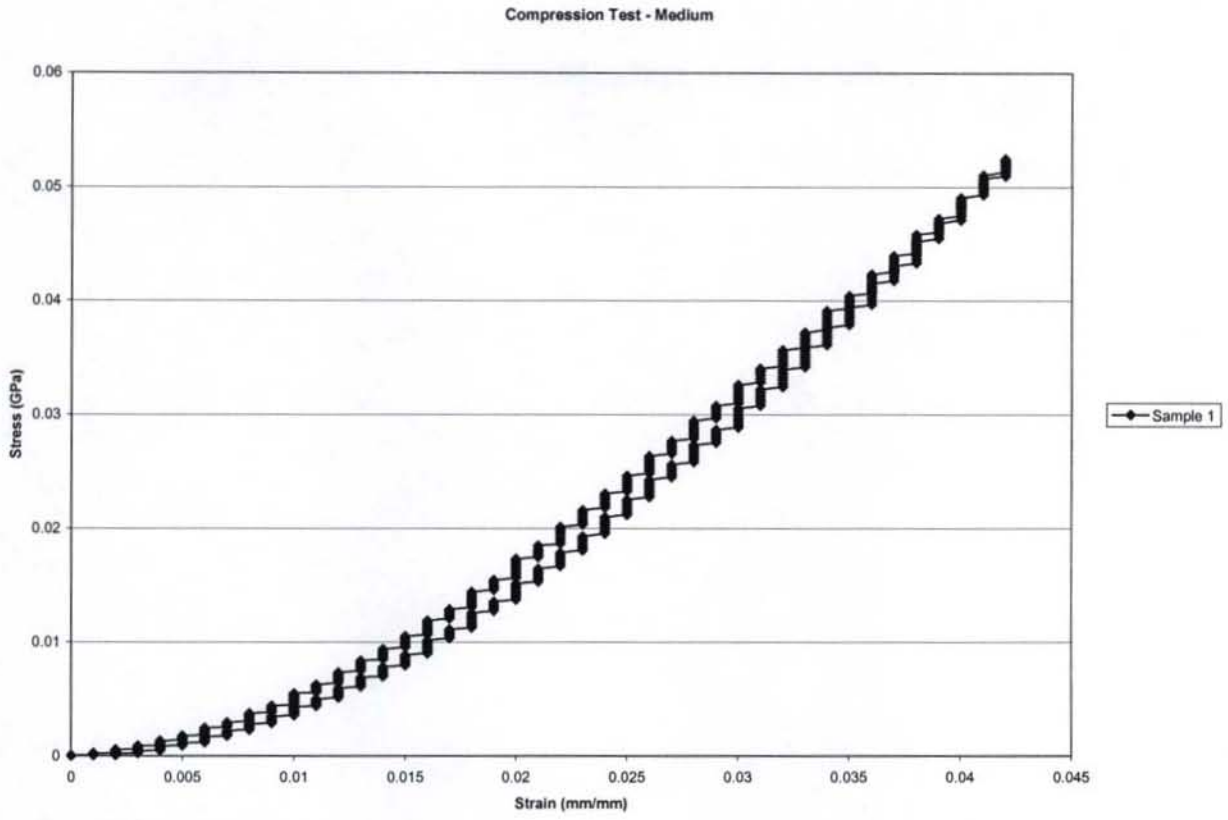

Figure 7- 6.15 mm thickness

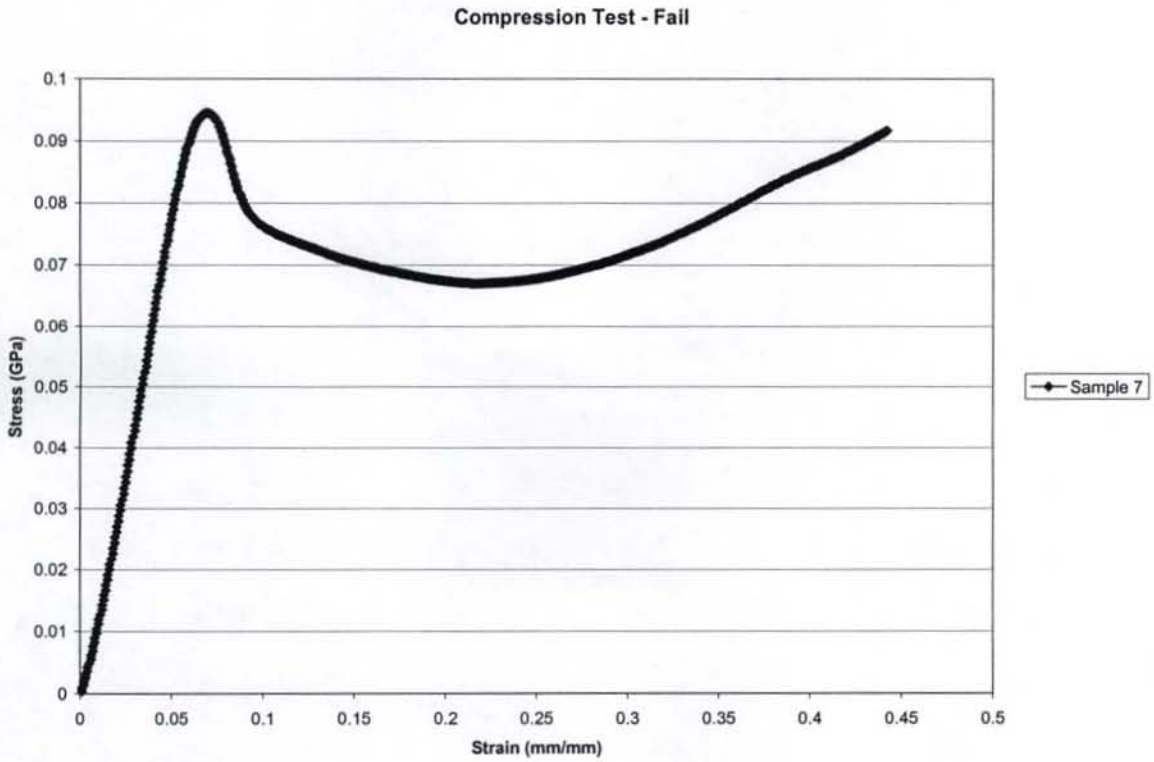

Figure 8 – 7.303 mm thickness

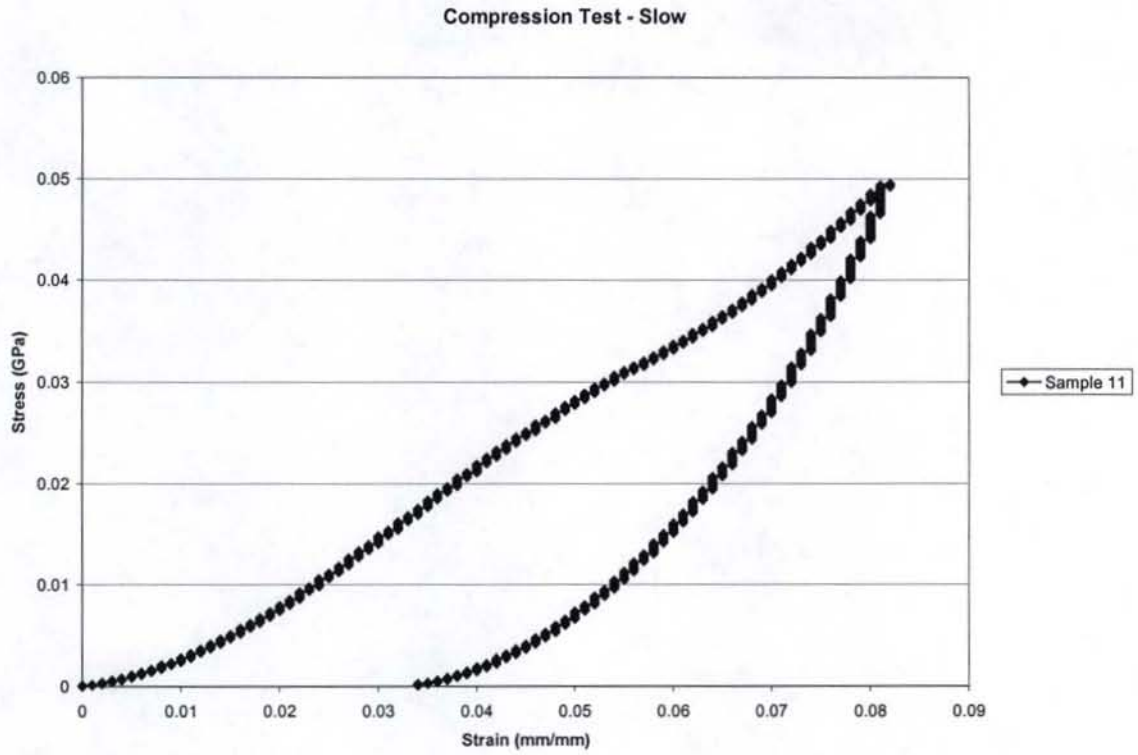

Figure 9 - 6.82 mm thickness

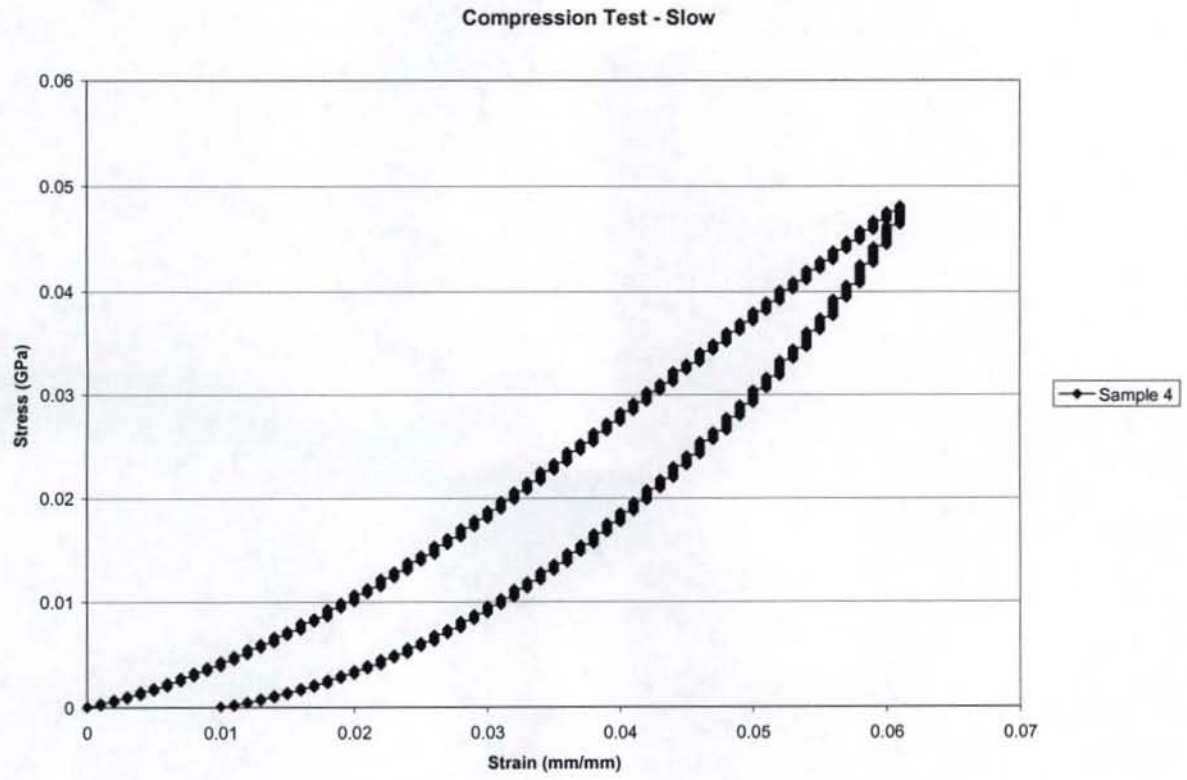

Figure 10 - 5.80 mm thickness

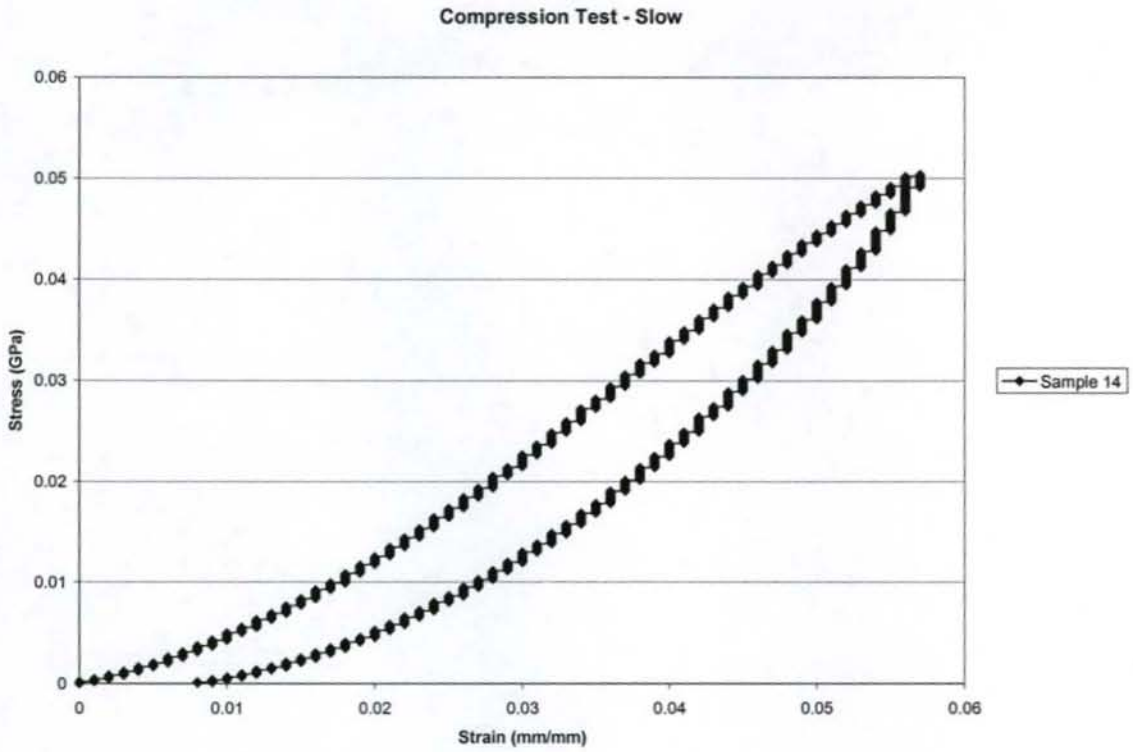

Figure 11 – 7.267 mm thickness

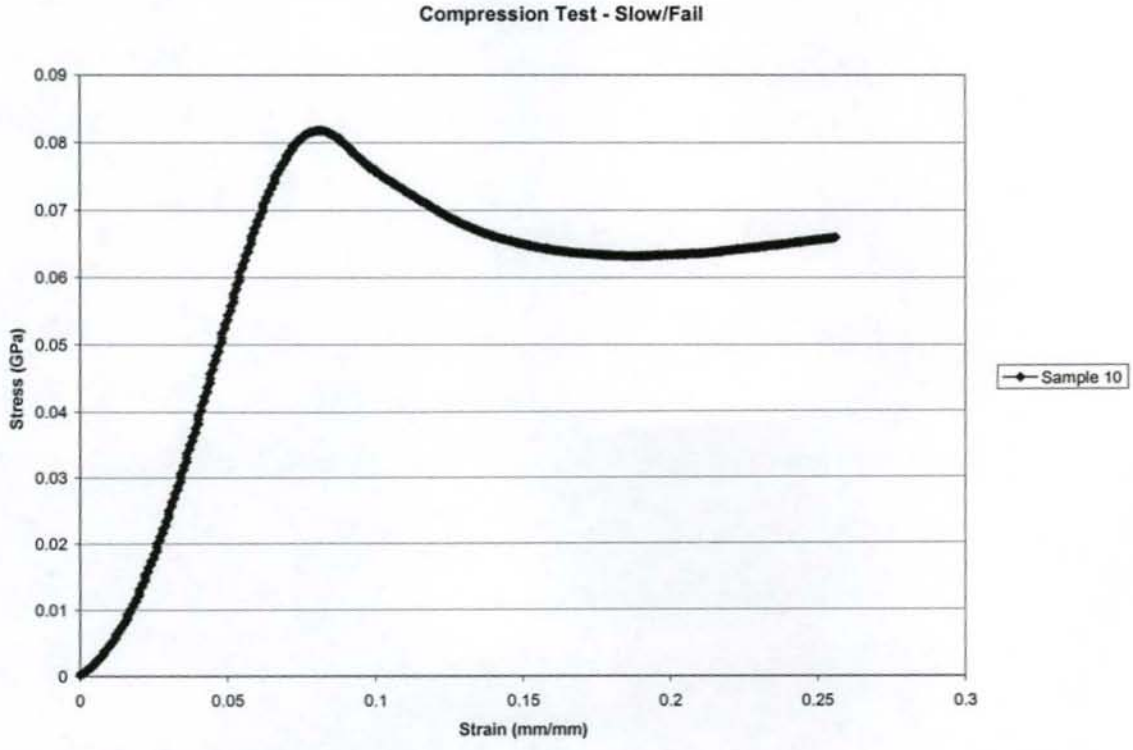

Figure 12 - 7.28 mm thickness